TECHNICAL UNIVERSITY OF CRETE | SCHOOL OF PRODUCTION ENGINEERING AND MANAGEMENT

A Comparative Analysis of Feedback and Feedforward Controllers for an Industrial Scale Heat Exchanger

Undergraduate Student: Kallergis Emmanouil

R.N.: 2018010054

Supervising professor: Dimitris Ipsakis

Chania, September 2025

Abstract

This thesis tackles the problem of dynamic modeling of a shell-and-tube heat exchanger as well as developing different strategies for its control. In essence, this study relates to control systems theory, a field within mathematics and engineering that focuses on analyzing the behavior of dynamic systems through the use of various controllers. It is widely known that most systems follow a non-linear pattern, making them difficult to interpret. Thus, the need of linearization arises. By differentiating the input and output with one differential equation each mathematical representation such as the Taylor Series, the Laplace Transformation and the State-Space model achieve a similar behavior (with minor deviations) . Doing so valuable information are drawn for the system such as its process transfer function. To develop practical designs for a variety of controllers a range of appropriate methodologies is applied. Those are the Ziegler–Nichols, the Tyreus-Luyben and the Morari-Zafiriou for a feedback control layout, while for a feedforward control layout one control system approach was introduced. Simulations and a comparative analysis followed in order to determine the best among these controllers for the heat exchanger. A total of seven controllers were used in the simulation scenarios. In more detail, the three controllers P, PI, PID by Ziegler–Nichols, the two controllers PI, PID by Tyreus-Luyben, the Morari-Zafiriou (model-based) and the feedforward controller were tuned and developed. Their comparison was performed under three different scenarios i) a steady reference signal, ii) a variable reference signal and iii) a steady reference signal with two disturbances (temperature of the inlet hot and cold streams). The results drawn from the simulations conclude that the most suitable controller for the heat exchanger is the one by Morari-Zafiriou methodology (model-based). It is the most robust among the seven, giving near zero error values while reaching the predetermined set point in minimal time. Right after follows the PID of the Ziegler–Nichols methodology as the second most appropriate for the control of the exchanger.

Περίληψη

Αυτή η διπλωματική εργασία ασχολείται με το πρόβλημα της δυναμικής μοντελοποίησης ενός εναλλάκτη θερμότητας κελύφους αυλών, καθώς και με την ανάπτυξη διαφορετικών στρατηγικών για τον έλεγχό του. Ουσιαστικά, η μελέτη αυτή σχετίζεται με τη θεωρία συστημάτων ελέγχου, έναν τομέα των μαθηματικών και της μηχανικής που εστιάζει στην ανάλυση της συμπεριφοράς δυναμικών συστημάτων μέσω της χρήσης διαφόρων ελεγκτών. Είναι ευρέως γνωστό ότι τα περισσότερα συστήματα ακολουθούν ένα μη γραμμικό πρότυπο, γεγονός που τα καθιστά δύσκολα στην χρήση. Έτσι, προκύπτει η ανάγκη γραμμικοποίησης τους. Με τη διαφοροποίηση της εισόδου και της εξόδου μέσω μιας διαφορικής εξίσωσης, κάθε μαθηματική αναπαράσταση όπως η ανάπτυξη σε σειρά Taylor, ο μετασχηματισμός Laplace και το μοντέλο χώρου καταστάσεων επιτυγχάνουν μια παρόμοια συμπεριφορά (με μικρές αποκλίσεις). Με αυτόν τον τρόπο εξάγονται πολύτιμες πληροφορίες για το σύστημα, όπως η συνάρτηση μεταφοράς της διεργασίας. Για την ανάπτυξη πρακτικών σχεδίων διάφορων ελεγκτών εφαρμόζεται μια σειρά από κατάλληλες μεθοδολογίες. Αυτές είναι οι Ziegler–Nichols, Tyreus-Luyben και Morari-Zafiriou για μία διάταξη ανάδρασης (feedback control), ενώ για μία διάταξη πρόδρασης (feedforward control) εισήχθει ένας ακόμα ελεγκτής. Οι τιμές απαραίτητες για τις μεθοδολογίες Ziegler–Nichols και Tyreus-Luyben βρέθηκαν μέσω της μεθόδου γεωμετρικού τόπου ρίζων. Ακολούθησαν προσομοιώσεις και συγκριτική ανάλυση με σκοπό τον προσδιορισμό του καταλληλότερου ελεγκτή για τον εναλλάκτη θερμότητας. Συνολικά επτά ελεγκτές χρησιμοποιήθηκαν στα σενάρια προσομοίωσης. Πιο συγκεκριμένα, οι ελεγκτές P, PI, PID από την μεθοδολογία Ziegler–Nichols, οι PI, PID από την μεθοδολογία Tyreus-Luyben, ο Morari-Zafiriou και ο feedforward, υποβλήθηκαν σε τρία διαφορετικά σενάρια: για ένα σταθερό σήμα αναφοράς, για ένα μεταβλητό σήμα αναφοράς, καθώς και για ένα σταθερό σήμα αναφοράς με την εισαγωγή δύο διαταραχών ($T_{in,hot}$, $T_{in,cold}$). Τα αποτελέσματα που προέκυψαν από τις προσομοιώσεις καταλήγουν στο ότι ο καταλληλότερος ελεγκτής για τον εναλλάκτη θερμότητας για την διάταξη ανάδρασης (feedback control), είναι αυτός της μεθοδολογίας Morari-Zafiriou. Ακολουθεί ο PID της Ziegler–Nichols ως δεύτερο, ο PID της Tyreus-Luyben ως τρίτος, οι PI και των δύο μεθοδολογιών με παρόμοια αποτελέσματα και τέλος ο P της Ziegler–Nichols ως ο πιο ακατάλληλος. Έπειτα ο Morari-Zafiriou συγκρίθηκε με τον ελεγκτή από την διάταξη πρόδρασης (feedforward control), όπου πάλι αποδείχτηκε ο πιο κατάλληλος. Είναι ο πιο αξιόπιστος ανάμεσα στους επτά, προσδίδει στο σύστημα ευστάθεια, εμφανίζοντας σχεδόν μηδενικά σφάλματα, ενώ ταυτόχρονα επιτυγχάνει το προκαθορισμένο σημείο αναφοράς σε ελάχιστο χρόνο για όλα τα σενάρια προσομοίωσης.

Table of Contents

Chapter 1

Introduction

Heat exchangers play a crucial role in various processes in today's industry, such as in processes related to power generation in chemical units, flue gas cooling, HVAC systems, power plants with steam generation and energy savings. As a process unit, it allows heat to be transferred between two or more fluids that can be in the form of liquids and/or gas without facing direct contact. Moreover, heat exchangers are a topic widely taught in engineering schools as it provides the basic principles regarding heat transferring from a hot stream to a cold stream in a confined environment that evolves in time. The most widely used types are a) shell and tube, b) plate heat exchangers, c) air cooled and d) double pipe. In all these types, there is a variation in the flow of the fluids and the related compartments.

Anxionnaz et al. [1] explores the concept of a heat exchanger reactor intensification in chemical engineering. The aim of the study is to combine heat exchange and reaction processes into a single unit. With this concept, a series of advantages such as increased efficiency, safety, and sustainability are achieved. Some other processes that the heat exchanger reactors are applicable to are polymerization, hydrogen production and oxidation reactions. More specifically in P. Kapustenko et al. paper [2] the use of plate heat exchangers is tested in regard to boosting energy efficiency in the production of phosphoric acid replacing the conventional tubular exchanger. Based on the results, it was found an improvement in process efficiency and a decrease in materials required for construction, (low total costs). Regarding power generation, a lot of industrial processes have energy wasted as heat. Having realized that Song Lv et al [3] compared different heat exchangers providing insights into the influence they have on the performance of thermoelectric generators. In this study they investigated the differences of three typical heat exchangers in a thermoelectric setup, and the power consumed by the auxiliary equipment to improve the thermoelectric performance. The property of a thermoelectric material is that it produces an electric current when it gets heated up. Furthermore, the performance of a thermoelectric generator depends on a significant temperature difference which is maintained by a heat exchanger. Another interesting topic is presented in [4]. D. S. Patil et al. stated that around 60 to 70% of fuel energy can be wasted as heat in an internal combustion engine. Hence, a thorough analysis on thermoelectric materials and heat exchangers for power generation was provided as a review study.

The main principles of a heat exchanger are shown in Fig. 1. As can be seen, two inputs (a hot and a cold) and two outputs (a hot and a cold) are combined but not coming in direct contact with. S. Padhee in [5] reveals that the shell-and-tube heat exchanger is most commonly used due to the wide range of temperature and pressure it can function on. This heat exchanger, as the name suggests, is an arrangement of tubes which are fastened inside a shell. One fluid runs through the tubes and the other through the shell.

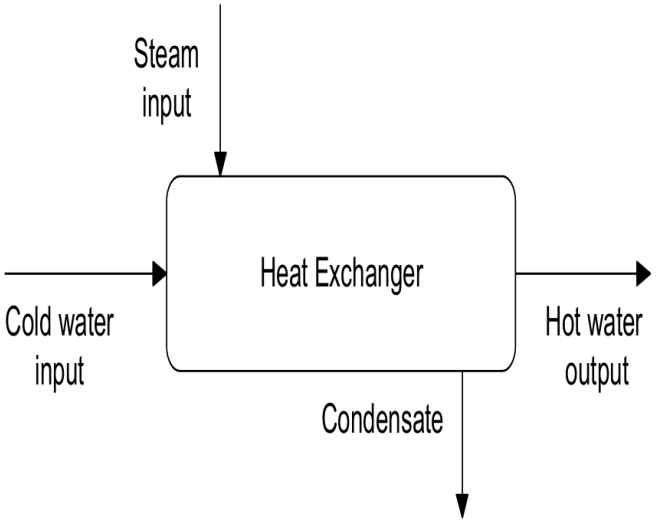

Figure 1.1: Principle of Heat Exchanger

There is a plethora of different types of heat exchangers which are classified based on construction, transfer process, flow arrangement and phase of liquid. A summary of these classifications is presented in figure 2.

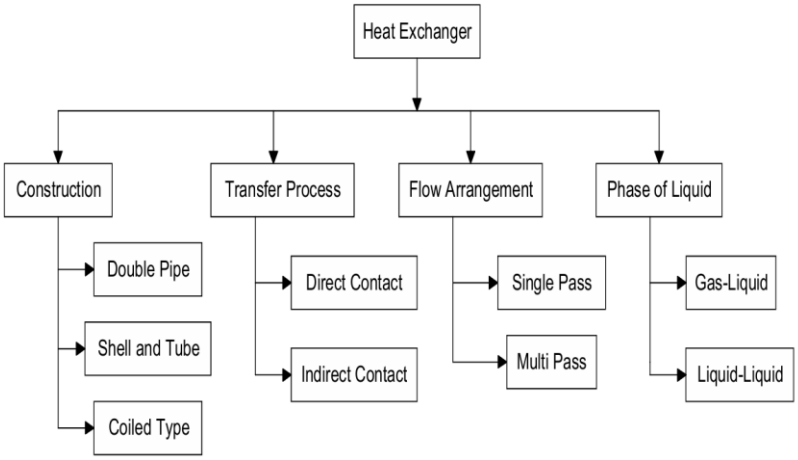

Figure 1.2: Classification of Heat Exchanger

As the concept of heat exchanger study is immense, this thesis will explore the options of modeling a shell and tube heat exchanger in the form of non-linear, linear and state-space model representation. The three types of models will be equivalent and will be provided as a basic structure of modeling. Next, the state-space model will lead to the respective transfer-functions that will "fuel" the control analysis in the former of conventional and advanced schemes. With this in mind, a brief literature review is provided.

The primary goal of researchers and engineers regarding heat exchangers is to minimize the time it takes for one fluid to reach a desired temperature by manipulating only the flow of the other. Meanwhile, the system has to maintain the required temperature despite disturbances (e.g. in the flow or temperature of the inlet streams). This led to the development of a wide variety of control strategies. S. I. Ao [6] compares a PID controller in a traditional feedback loop, a feedforward controller implemented alongside the PID and a hybrid PID controller that utilizes fuzzy logic. The results suggest that the fuzzy PID outperforms the other two controllers. In [7], R. Ranjan and S. Kumar focused on enhancing the performance of a heat exchanger with the use of a Nonlinear Model Predictive Controller that utilizes fuzzy logic (NMPC-FO) as well. The outcome of the optimization is an improvement in energy efficiency, reduction of cost and a reduced fouling rate in comparison to other conventional strategies. E. Tridianto et al. [8] developed a cascaded PID controller modeled as a First Order Plus Delay Time system (FOPDT), aiming to improve the temperature control of a heat exchanger. The best performance observed was from a PID controller in the main loop and a PI controller in the secondary loop. The system could regulate the temperature regardless of the flow state of the fluids with minimal integral absolute error. S. Padhee [5] compares feedback, feedforward plus feedback and Integral Model Control (IMC) for temperature regulation in a shell-and-tube heat exchanger. The simulations done conclude that the IMC achieved a superior performance against the other two. R. Dyrska et al. [9] proposed a more advanced control scheme. Specifically, the study worked on a modified Model Predictive Controller for a plate heat exchanger. This control method reduced computational efforts by removing inactive constraints while maintaining temperature control. The modified constraint removal approach achieved the robustness required for a practical application to a laboratory-scaled heat exchanger as analyzed from the industrial perspective. Getting slightly more generic, L. Liu [10] presents a review of some industrial applications of feedforward control. He focuses on two distinct objectives this kind of control excels at, disturbance rejection and reference tracking. Furthermore, tuning methods are suggested for both objectives. Y. Fürst et al. [11] introduced a nonlinear modeling approach for heat exchangers. The conventional strategies used fall short when it comes to real world changes. Results yielded by simulations done to the system showed an accurate representation of the heat exchangers dynamic. B. Tomar et al. [12] dives into intelligent control strategies, specifically in the use of Programmable Logic Controllers (PLC) and Supervisory Control and Data Acquisition (SCADA) systems. A Fractional-Order PID (FOPID) controller was finely tuned using genetic algorithms (GA) and particle swarm optimization (PSO). Experimental data concludes that the application of PLC and SCADA systems enhances the efficiency and precision of temperature control, in comparison to a standard PID.

The core focus of this study is to compare the feedback and feedforward control for temperature regulation in a traditional shell and tube heat exchanger.

.

Chapter 2

Mathematical Analysis and Linearization of the Heat Exchanger

In the present chapter, the development of the mathematical model for the shell-tube heat exchanger system is presented. As will be discussed, this model will be developed in a non-linear form and then it will be linearized towards a state-space representation. In order to verify the suitability of the models, the results of the linear models along with the nonlinear (derived from MATLAB codes) are going to be presented through comprehensive diagrams.

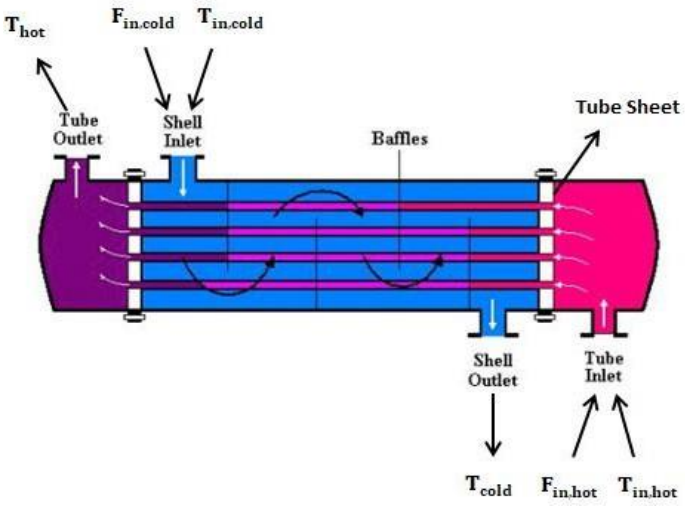

Figure 2.1: Input and output variables for a simple shell-and-tube heat exchanger

As is observed in the above figure, there are two flow channels (compartments). One channel refers to the flow through the shell-side and the other through the tube-side. The cold flow corresponds to the shell side channel, while the hot to the tube side channel. It is established that the shell inlet has two input variables called $F_{in,cold}$ and $T_{in,cold}$. $F_{in,cold}$ refers to the flow rate at the inlet of the cold liquid in the shell of the exchanger and $T_{in,cold}$ refers to the inlet temperature of the cold liquid in the shell (will be used later as a disturbance). At the shell outlet there is an output variable T_{cold} referring to the temperature of the cold flow exiting the shell. Furthermore, at the tube inlet, there are two input variables called $F_{in,hot}$ and $T_{in,hot}$. $F_{in,hot}$ refers to the flow rate at the inlet of the hot liquid in the tubes of the exchanger and $T_{in,hot}$ refers to the inlet temperature of the hot liquid in the tubes (will be used later as a disturbance). At the tube outlet is an output variable T_{hot} referring to the temperature of the hot flow exiting the tubes.

2.1 Mathematical Modeling of a Shell-and-Tube Heat Exchanger

The following mathematical modeling is the analytical expression from source [13]. The development of the mathematical model employed fundamental laws of physics and important relations from the following sources [14], [15]. Finally, similar mathematical models (based on experimental measurements) for this specific heat exchanger system were found in literature studies [16], [5].

Mass Balance:

$$\frac{d(V*\rho)}{dt} = \sum F_{in} \cdot \rho - \sum F_{out} \cdot \rho \qquad (2.1)$$

For constant density, equation (2.1) becomes:

$$\frac{dV}{dt} = \sum F_{in} - \sum F_{out} \qquad (2.2)$$

The sum of the flow rates entering the system is equal to the sum of the flow rates exiting it:

$$\sum F_{in} = \sum F_{out} \qquad (2.3)$$

Energy Balance:

$$\frac{dE}{dt} = \frac{d(U+K+P)}{dt} = \sum F_{in} \cdot \rho \cdot \left(\bar{H}_{in} + \frac{u^2}{2} + g \cdot z\right) - \sum F_{out} \cdot \rho \cdot \left(\bar{H}_{out} + \frac{u^2}{2} + g \cdot z\right) + Q + W \qquad (2.4)$$

$$H = U + p \cdot V \qquad (2.5)$$

$$Q = U \cdot A \cdot \Delta T \Rightarrow Q = U \cdot A \cdot (T_{in} - T_{out}) \qquad (2.6)$$

Assumptions for equations (2.4), (2.5):

- The kinetic and potential energy is not taken into account.
- W=0 for the system work.
- $\frac{d(V \cdot \rho)}{dt} \Rightarrow 0$, negligible quantity.

Equation (2.4), after the assumptions and the contribution of equations (2.5) and (2.6), transforms into:

$$\frac{dH}{dt} = \sum F_{in} \cdot \rho \cdot \bar{H}_{in} - \sum F_{out} \cdot \rho \cdot \bar{H}_{out} + U \cdot A(T_{cold} - T_{hot}) \quad (2.7)$$

Total Enthalpy: $H = V \cdot \rho \cdot \bar{H}$ (2.8)

Another assumption is that there is no phase change.

$$\bar{H}(T) = \int_{T_{ref}}^{T} c_p \, dT \quad (2.9)$$

Equation (2.7), with the contribution of equations (2.8) and (2.9), becomes:

$$\frac{d\left(V \cdot \rho \cdot c_p \cdot (Thot - T_{ref})\right)}{dt} = \sum F_{in} \cdot \rho \cdot c_p \cdot \left(T_{in} - T_{ref}\right) - \sum F_{out} \cdot \rho \cdot c_p \cdot \left(T_{hot} - T_{ref}\right) + U \cdot A \cdot (T_{cold} - T_{hot}) \quad (2.10)$$

Analyzing the derivative of the first term and after performing calculations, as some terms are eliminated, equation (2.10) is as follows:

$$V \cdot \rho \cdot c_\rho \cdot \frac{d(T_{hot} - Tref)}{dt} = \sum F_{in} \cdot \rho \cdot c_p \cdot (T_{in} - T_{hot}) + U \cdot A \cdot (T_{cold} - T_{hot}) \quad (2.11a)$$

$$V \cdot \rho \cdot c_\rho \cdot \frac{d(T_{cold} - Tref)}{dt} = \sum F_{in} \cdot \rho \cdot c_p \cdot (T_{in} - T_{cold}) - U \cdot A \cdot (T_{cold} - T_{hot}) \quad (2.11b)$$

If it is assumed that in the system T_{ref} is constant and that we are considering two flows in the heat exchanger (hot and cold), the following equations are created:

$$\frac{dV_{hot}}{dt} = F_{in} - F_{out} \quad (2.12)$$

$$\frac{dT_{hot}}{dt} = \frac{F_{in,hot,s}}{V_{hot,s}} \cdot \left(T_{in,hot,s} - T_{hot}\right) + \frac{U \cdot A \cdot (T_{cold} - T_{hot})}{V_{hot,s} \cdot \rho_{hot} \cdot c_{p,hot}} \quad (2.13) \textbf{ (hot flow)}$$

Similarly, for the cold stream, we have a small change in the sign of the heat, and where the "hot" index is replaced by the "cold" index.

$$\frac{dV_{cold}}{dt} = F_{in} - F_{out} \quad (2.14)$$

$$\frac{dT_{cold}}{dt} = \frac{F_{in,cold,s}}{V_{cold,s}} \cdot \left(T_{in,cold,s} - T_{cold}\right) - \frac{U \cdot A \cdot (T_{cold} - T_{hot})}{V_{cold,s} \cdot \rho_{cold} \cdot c_{p,cold}} \quad (2.15) \textbf{ (cold flow)}$$

The index “s” indicates that the variables are constants.

2.2 Linearization of the Shell-and-Tube Heat Exchanger System

From the modeling done on the system, which was analyzed in the previous subsection, the following relations were formulated:

$$\frac{dT_{hot}}{dt} = \frac{F_{in,hot,s}}{V_{hot,s}} \cdot \left(T_{in,hot,s} - T_{hot}\right) + \frac{U \cdot A \cdot (T_{cold} - T_{hot})}{V_{hot,s} \cdot \rho_{hot} \cdot c_{p,hot}} \qquad (2.13) \text{ (hot flow)}$$

$$\frac{dT_{cold}}{dt} = \frac{F_{in,cold,s}}{V_{cold,s}} \cdot \left(T_{in,cold,s} - T_{cold}\right) - \frac{U \cdot A \cdot (T_{cold} - T_{hot})}{V_{cold,s} \cdot \rho_{cold} \cdot c_{p,cold}} \qquad (2.15) \text{ (cold flow)}$$

As observed, (2.13) and (2.15) referring to the two flows of the heat exchanger are nonlinear differential equations. For instance, the input of the hot flow $F_{in,hot}$ is multiplied by the disturbance $T_{in,hot}$, the same happens for the cold flow. To facilitate the study of this specific system and to extract information from it, the system must be linearized. For the linearization, the state-space model will be used, along with the Taylor series and the Laplace transform.

2.2.1 Linearization - Taylor Series

Firstly, for the linearization of the nonlinear differential equations the Taylor series expansion around a steady-state point $x(t_s)= x_s$, at which the derivative is zero ($\frac{dx(t_s)}{dt} = 0$). The Taylor series expansion method for linearizing the system is consistent with the author of source [17].

For the hot flow

$$\frac{dT_{hot}}{dt} = (SS) - \left[\frac{F_{in,hot}}{V_{hot}}\right]_s \cdot \left(T_{hot} - T_{hot,s}\right) - \left[\frac{U \cdot A}{\rho_{hot} \cdot c_{p,hot} \cdot V_{hot}}\right]_s \cdot \left(T_{hot} - T_{hot,s}\right) + \left[\frac{U \cdot A}{\rho_{hot} \cdot c_{p,hot} \cdot V_{hot}}\right]_s \cdot \left(T_{cold} - T_{cold,s}\right) + \left[\frac{T_{in,hot}}{V_{hot}}\right]_s \cdot \left(F_{in,hot} - F_{in,hot,s}\right) - \left[\frac{T_{hot}}{V_{hot}}\right]_s \cdot \left(F_{in,hot} - F_{in,hot,s}\right) + \left[\frac{F_{in,hot}}{V_{hot}}\right]_s \cdot \left(T_{in,hot} - T_{in,hot,s}\right) \qquad (2.16)$$

The terms inside the parentheses (e.g., $T_{hot} - T_{hot,s}$, $F_{in,hot} - F_{in,hot,s}$) are called deviation variables around a point $x(t_s)= x_s$. The steady-state point is $T_{hot,s}$= 375 K and its derivative is (SS)=0, so equation (2.16) becomes:

$$\frac{dT_{hot}}{dt} = \frac{d(T_{hot} - T_{hot,s})}{dt} = -\left[\frac{F_{in,hot}}{V_{hot}} + \frac{U \cdot A}{\rho_{hot} \cdot c_{p,hot} \cdot V_{hot}}\right]_s \cdot \left(T_{hot} - T_{hot,s}\right) + \left[\frac{U * A}{\rho_{hot} * c_{p,hot} * V_{hot}}\right]_s \cdot \left(T_{cold} - T_{cold,s}\right) + \left[\frac{(T_{in,hot} - T_{hot})}{V_{hot}}\right]_s \cdot \left(F_{in,hot} - F_{in,hot,s}\right) + \left[\frac{F_{in,hot}}{V_{hot}}\right]_s \cdot \left(T_{in,hot} - T_{in,hot,s}\right) \qquad (2.17)$$

For the cold flow

$$\frac{dT_{cold}}{dt} = (SS) - \left[\frac{F_{in,cold}}{V_{cold}}\right]_s \cdot \left(T_{cold} - T_{cold,s}\right) - \left[\frac{U \cdot A}{\rho_{cold} \cdot c_{p,cold} \cdot V_{cold}}\right]_s * \left(T_{cold} - T_{cold,s}\right) + \left[\frac{U \cdot A}{\rho_{cold} \cdot c_{p,cold} \cdot V_{cold}}\right]_s \cdot \left(T_{hot} - T_{hot,s}\right) + \left[\frac{T_{in,cold}}{V_{cold}}\right]_s \cdot \left(F_{in,cold} - F_{in,cold,s}\right) - \left[\frac{T_{cold}}{V_{cold}}\right]_s \cdot \left(F_{in,cold} - F_{in,cold,s}\right) + \left[\frac{F_{in,cold}}{V_{cold}}\right]_s \cdot \left(T_{in,cold} - T_{in,cold,s}\right) \quad (2.18)$$

The terms inside the parentheses (e.g., $T_{cold} - T_{cold,s}$, $F_{in,cold} - F_{in,cold,s}$) are called deviation variables around a point $x(t_s) = x_s$. The steady-state point is $T_{cold,s}$= 320 K and its derivative is (SS)=0, so equation (2.18) becomes:

$$\frac{dT_{cold}}{dt} = \frac{d(T_{cold} - T_{cold,s})}{dt} = -\left[\frac{F_{in,cold}}{V_{cold}} + \frac{U \cdot A}{\rho_{cold} \cdot c_{p,cold} \cdot V_{cold}}\right]_s \cdot \left(T_{cold} - T_{cold,s}\right) + \left[\frac{U \cdot A}{\rho_{cold} \cdot c_{p,cold} \cdot V_{cold}}\right]_s \cdot \left(T_{hot} - T_{hot,s}\right) + \left[\frac{(T_{in,cold} - T_{cold})}{V_{cold}}\right]_s \cdot \left(F_{in,cold} - F_{in,cold,s}\right) + \left[\frac{F_{in,cold}}{V_{cold}}\right]_s \cdot \left(T_{in,cold} - T_{in,cold,s}\right) \quad (2.19)$$

2.2.2 Linearization – State Space Model

The linear differential equations in the time domain must be formulated into the following general form that characterizes the state space model:

$$\dot{x}(t) = A \cdot x(t) + B \cdot u(t) + E \cdot d(t)$$

$$y(t) = C \cdot x(t) + D \cdot u(t)$$

Where:

- x: state variables (T_{hot} , T_{cold})
- y: output variables (T_{hot} , T_{cold})
- u: input variables ($F_{in,hot}$, $F_{in,cold}$)
- d: disturbances ($T_{in,hot}$, $T_{in,cold}$)

A, B, C, D, E are state space matrices that fully describe the model.

This specific form is another alternative linearization of the nonlinear model, according to the author of source [18].

$$\begin{bmatrix} \dot{T'}_{hot} \\ \dot{T'}_{cold} \end{bmatrix} = \overset{A}{\begin{bmatrix} -\left[\frac{F_{in,hot}}{V_{hot}} + \frac{U \cdot A}{\rho_{hot} \cdot c_{p,hot} \cdot V_{hot}}\right]_s & \left[\frac{U \cdot A}{\rho_{hot} \cdot c_{p,hot} \cdot V_{hot}}\right]_s \\ \left[\frac{U \cdot A}{\rho_{cold} \cdot c_{p,cold} \cdot V_{cold}}\right]_s & -\left[\frac{F_{in,cold}}{V_{cold}} + \frac{U \cdot A}{\rho_{cold} \cdot c_{p,cold} \cdot V_{cold}}\right]_s \end{bmatrix}} \cdot \begin{bmatrix} T'_{hot} \\ T'_{cold} \end{bmatrix} +$$

$$\overset{B}{\begin{bmatrix} \left[\frac{(T_{in,hot} - T_{hot})}{V_{hot}}\right]_s & 0 \\ 0 & \left[\frac{(T_{in,cold} - T_{cold})}{V_{cold}}\right]_s \end{bmatrix}} \cdot \begin{bmatrix} F'_{in,hot} \\ F'_{in,cold} \end{bmatrix} + \overset{E}{\begin{bmatrix} \left[\frac{F_{in,hot}}{V_{hot}}\right]_s & 0 \\ 0 & \left[\frac{F_{in,cold}}{V_{cold}}\right]_s \end{bmatrix}} \cdot \begin{bmatrix} T'_{in,hot} \\ T'_{in,cold} \end{bmatrix}$$

(2.20)

$$\begin{bmatrix} T_{hot} \\ T_{cold} \end{bmatrix} = \overset{C}{\begin{bmatrix} 1 & 0 \\ 0 & 1 \end{bmatrix}} \cdot \begin{bmatrix} T'_{hot} \\ T'_{cold} \end{bmatrix} + \overset{D}{\begin{bmatrix} 0 & 0 \\ 0 & 0 \end{bmatrix}} \cdot \begin{bmatrix} F'_{in,hot} \\ F'_{in,cold} \end{bmatrix} \qquad (2.21)$$

The state, output, input, and disturbance variables with a prime (e.g., T'_{hot}) represent the deviation variables around a point $x(t_s) = x_s$ .For instance, $T'_{hot} = (T_{hot} - T_{hot,s})$.

Also, from the state space model matrices, the process transfer function of the system (Gp) can be calculated, which is very important information, as it will later be used in the closed-loop system alongside the controllers.

The transfer function can be calculated using the equation below.

$$Gp = \frac{y(s)}{u(s)} = [C \cdot (s \cdot I - A)^{-1} \cdot B + D] \qquad (2.22)$$

After performing calculations and using the state space model matrices (2.20) and (2.21), the transfer function (2.22) is derived as follows:

Gp=

$$\begin{bmatrix} \frac{s + \left[\frac{F_{in,cold}}{V_{cold}} + \frac{U \cdot A}{\rho_{cold} \cdot c_{p,cold} \cdot V_{cold}}\right]_s \cdot \left[\frac{(T_{in,hot} - T_{hot})}{V_{hot}}\right]_s}{\det(s \cdot I - A)} & \frac{\left[\frac{U \cdot A}{\rho_{hot} \cdot c_{p,hot} \cdot V_{hot}}\right]_s \cdot \left[\frac{(T_{in,cold} - T_{cold})}{V_{cold}}\right]_s}{\det(s * I - A)} \\ \frac{\left[\frac{U \cdot A}{\rho_{cold} \cdot c_{p,cold} \cdot V_{cold}}\right]_s \cdot \left[\frac{(T_{in,hot} - T_{hot})}{V_{hot}}\right]_s}{\det(s \cdot I - A)} & \frac{s + \left[\frac{F_{in,hot}}{V_{hot}} + \frac{U \cdot A}{\rho_{hot} \cdot c_{p,hot} \cdot V_{hot}}\right]_s \cdot \left[\frac{(T_{in,cold} - T_{cold})}{V_{cold}}\right]_s}{\det(s \cdot I - A)} \end{bmatrix}$$

(2.23)

The first element of equation (2.23), matrix (1,1) represents the response of T_{hot} with respect to the system input $F_{in,hot}$. The matrix element (2,1) represents the response of T_{hot} with respect to the input $F_{in,cold}$. The element (1,2) indicates the response of T_{cold} with respect to the input $F_{in,hot}$. Finally, the element (2,2) represents the response of T_{cold} with respect to the input $F_{in,cold}$.

The most important relationship among the matrix elements is (2,1), as in the closed-loop system with a controller, this specific process transfer function is located within the closed loop.

2.2.3 Linearization – Laplace Transform

Equations (2.17) and (2.19) will be transformed from the domain of time (t) to the Laplace domain (s). This is another way of expressing the system's linearization, providing the analytical expressions for the two responses of the heat exchanger, $T'_{hot}(s)$ and $T'_{cold}(s)$. The Laplace transform methodology, which is analyzed below, is in accordance with source [17].

For the hot flow

The starting temperature of the hot flow is 423 K (at t=0).

$$s \cdot T'_{hot}(s) - \cancel{T'_{hot}(0)}^{423K} = -\left[\frac{F_{in,hot}}{V_{hot}} + \frac{U \cdot A}{\rho_{hot} \cdot c_{p,hot} \cdot V_{hot}}\right]_s \cdot T'_{hot}(s) + \left[\frac{U \cdot A}{\rho_{hot} \cdot c_{p,hot} \cdot V_{hot}}\right]_s \cdot T'_{cold}(s) + \left[\frac{(T_{in,hot} - T_{hot})}{V_{hot}}\right]_s \cdot F'_{in,hot}(s) + \left[\frac{F_{in,hot}}{V_{hot}}\right]_s \cdot T'_{in,hot}(s) \quad (2.24)$$

After analyzing equation (2.24), the following result is obtained:

$$T'_{hot}(s) = \frac{\left[\frac{U \cdot A}{\rho_{hot} \cdot c_{p,hot} \cdot V_{hot}}\right]_s}{\left[s + \left(\frac{F_{in,hot}}{V_{hot}} + \frac{U \cdot A}{\rho_{hot} \cdot c_{p,hot} \cdot V_{hot}}\right)_s\right]} \cdot T'_{cold}(s) + \frac{\left[\frac{(T_{in,hot} - T_{hot})}{V_{hot}}\right]_s}{\left[s + \left(\frac{F_{in,hot}}{V_{hot}} + \frac{U \cdot A}{\rho_{hot} \cdot c_{p,hot} \cdot V_{hot}}\right)_s\right]} \cdot F'_{in,hot}(s) + \frac{\left[\frac{F_{in,hot}}{V_{hot}}\right]_s}{\left[s + \left(\frac{F_{in,hot}}{V_{hot}} + \frac{U \cdot A}{\rho_{hot} \cdot c_{p,hot} \cdot V_{hot}}\right)_s\right]} \cdot T'_{in,hot}(s) + \frac{423}{\left[s + \left(\frac{F_{in,hot}}{V_{hot}} + \frac{U \cdot A}{\rho_{hot} \cdot c_{p,hot} \cdot V_{hot}}\right)_s\right]}$$

(2.25)

For the cold flow

$$s \cdot T'_{cold}(s) - \cancel{T'_{cold}(0)}^{298K} = -\left[\frac{F_{in,cold}}{V_{cold}} + \frac{U \cdot A}{\rho_{cold} \cdot c_{p,cold} \cdot V_{cold}}\right]_s \cdot T'_{cold}(s) + \left[\frac{U \cdot A}{\rho_{cold} \cdot c_{p,cold} \cdot V_{cold}}\right]_s \cdot T'_{hot}(s) + \left[\frac{(T_{in,cold} - T_{cold})}{V_{cold}}\right]_s \cdot F'_{in,cold}(s) + \left[\frac{F_{in,cold}}{V_{cold}}\right]_s \cdot T'_{in,cold}(s) \quad (2.26)$$

After analyzing equation (2.26), the following result is obtained:

$$T'_{cold}(s) = \frac{\left[\frac{U \cdot A}{\rho_{cold} \cdot c_{p,cold} \cdot V_{cold}}\right]_s}{\left[s + \left(\frac{F_{in,cold}}{V_{cold}} + \frac{U \cdot A}{\rho_{cold} \cdot c_{p,cold} \cdot V_{cold}}\right)_s\right]} \cdot T'_{hot}(s) + \frac{\left[\frac{(T_{in,cold} - T_{cold})}{V_{cold}}\right]_s}{\left[s + \left(\frac{F_{in,cold}}{V_{cold}} + \frac{U \cdot A}{\rho_{cold} \cdot c_{p,cold} \cdot V_{cold}}\right)_s\right]} \cdot F'_{in,cold}(s) + \frac{\left[\frac{F_{in,cold}}{V_{cold}}\right]_s}{\left[s + \left(\frac{F_{in,cold}}{V_{cold}} + \frac{U \cdot A}{\rho_{cold} \cdot c_{p,cold} \cdot V_{cold}}\right)_s\right]} \cdot T'_{in,cold}(s) + \frac{298}{\left[s + \left(\frac{F_{in,cold}}{V_{cold}} + \frac{U \cdot A}{\rho_{cold} \cdot c_{p,cold} \cdot V_{cold}}\right)_s\right]} \quad (2.27)$$

By substituting equation (2.27) into equation (2.25), the following results:

$$T'_{hot}(s) = \rightarrow Gp\_F_{in,cold}(s)$$

$$\frac{\left[\frac{U*A}{\rho_{hot}*c_{p,hot}*V_{hot}}\right]_s * \left[\frac{(T_{in,cold} - T_{cold})}{V_{cold}}\right]_s}{\left[s + \left(\frac{F_{in,hot}}{V_{hot}} + \frac{U*A}{\rho_{hot}*c_{p,hot}*V_{hot}}\right)_s\right] * \left[s + \left(\frac{F_{in,cold}}{V_{cold}} + \frac{U*A}{\rho_{cold}*c_{p,cold}*V_{cold}}\right)_s\right] - \left[\frac{(U*A)^2}{(\rho_{hot}*c_{p,hot}*V_{hot})*(\rho_{cold}*c_{p,cold}*V_{cold})}\right]_s}$$

$$*F'_{in,cold}(s) +$$

$$\rightarrow Gp\_T_{in,cold}(s)$$

$$\frac{\left[\frac{U*A}{\rho_{hot}*c_{p,hot}*V_{hot}}\right]_s * \left[\frac{F_{in,cold}}{V_{cold}}\right]_s}{\left[s + \left(\frac{F_{in,hot}}{V_{hot}} + \frac{U*A}{\rho_{hot}*c_{p,hot}*V_{hot}}\right)_s\right] * \left[s + \left(\frac{F_{in,cold}}{V_{cold}} + \frac{U*A}{\rho_{cold}*c_{p,cold}*V_{cold}}\right)_s\right] - \left[\frac{(U*A)^2}{(\rho_{hot}*c_{p,hot}*V_{hot})*(\rho_{cold}*c_{p,cold}*V_{cold})}\right]_s}$$

$$*T'_{in,cold}(s) +$$

$$\rightarrow Gp_2(s)$$

$$\frac{\left[\frac{U*A}{\rho_{hot}*c_{p,hot}*V_{hot}}\right]_s * 298}{\left[s + \left(\frac{F_{in,hot}}{V_{hot}} + \frac{U*A}{\rho_{hot}*c_{p,hot}*V_{hot}}\right)_s\right] * \left[s + \left(\frac{F_{in,cold}}{V_{cold}} + \frac{U*A}{\rho_{cold}*c_{p,cold}*V_{cold}}\right)_s\right] - \left[\frac{(U*A)^2}{(\rho_{hot}*c_{p,hot}*V_{hot})*(\rho_{cold}*c_{p,cold}*V_{cold})}\right]_s}$$

+

$$\frac{\left[\frac{(T_{in,hot}-T_{hot})}{V_{hot}}\right]_s * \left[s+\left(\frac{F_{in,cold}}{V_{cold}}+\frac{U*A}{\rho_{cold}*c_{p,cold}*V_{cold}}\right)_s\right]}{\left[s+\left(\frac{F_{in,hot}}{V_{hot}}+\frac{U*A}{\rho_{hot}*c_{p,hot}*V_{hot}}\right)_s\right]*\left[s+\left(\frac{F_{in,cold}}{V_{cold}}+\frac{U*A}{\rho_{cold}*c_{p,cold}*V_{cold}}\right)_s\right]-\left[\frac{(U*A)^2}{(\rho_{hot}*c_{p,hot}*V_{hot})*(\rho_{cold}*c_{p,cold}*V_{cold})}\right]_s} \rightarrow Gp\_F_{in,hot}(s)$$

$$*F'_{in,hot}(s) +$$

$$\frac{\left[\frac{F_{in,hot}}{V_{hot}}\right]_s * \left[s+\left(\frac{F_{in,cold}}{V_{cold}}+\frac{U*A}{\rho_{cold}*c_{p,cold}*V_{cold}}\right)_s\right]}{\left[s+\left(\frac{F_{in,hot}}{V_{hot}}+\frac{U*A}{\rho_{hot}*c_{p,hot}*V_{hot}}\right)_s\right]*\left[s+\left(\frac{F_{in,cold}}{V_{cold}}+\frac{U*A}{\rho_{cold}*c_{p,cold}*V_{cold}}\right)_s\right]-\left[\frac{(U*A)^2}{(\rho_{hot}*c_{p,hot}*V_{hot})*(\rho_{cold}*c_{p,cold}*V_{cold})}\right]_s} \rightarrow Gp\_T_{in,hot}(s)$$

$$*T'_{in,hot}(s) +$$

$$\frac{\left[s+\left(\frac{F_{in,cold}}{V_{cold}}+\frac{U*A}{\rho_{cold}*c_{p,cold}*V_{cold}}\right)_s\right]*423}{\left[s+\left(\frac{F_{in,hot}}{V_{hot}}+\frac{U*A}{\rho_{hot}*c_{p,hot}*V_{hot}}\right)_s\right]*\left[s+\left(\frac{F_{in,cold}}{V_{cold}}+\frac{U*A}{\rho_{cold}*c_{p,cold}*V_{cold}}\right)_s\right]-\left[\frac{(U*A)^2}{(\rho_{hot}*c_{p,hot}*V_{hot})*(\rho_{cold}*c_{p,cold}*V_{cold})}\right]_s} \rightarrow Gp_1(s)$$

(2.28)

Equation (2.28) is the analytical expression of the response of the hot flow in the complex Laplace domain $T'_{hot}(s)$, which depends on the system's disturbances ($T'_{in,hot}(s)$, $T'_{in,cold}(s)$), the system inputs ($F'_{in,hot}(s)$, $F'_{in,cold}(s)$) and a constant that results from the Laplace transform of the derivatives of the hot and cold flow temperatures ($\frac{dT_{hot}}{dt}$ and $\frac{dT_{cold}}{dt}$). Arrows are used to highlight the transfer functions in their analytical form.

A corresponding equation is (2.27), which refers to the cold stream of the heat exchanger.

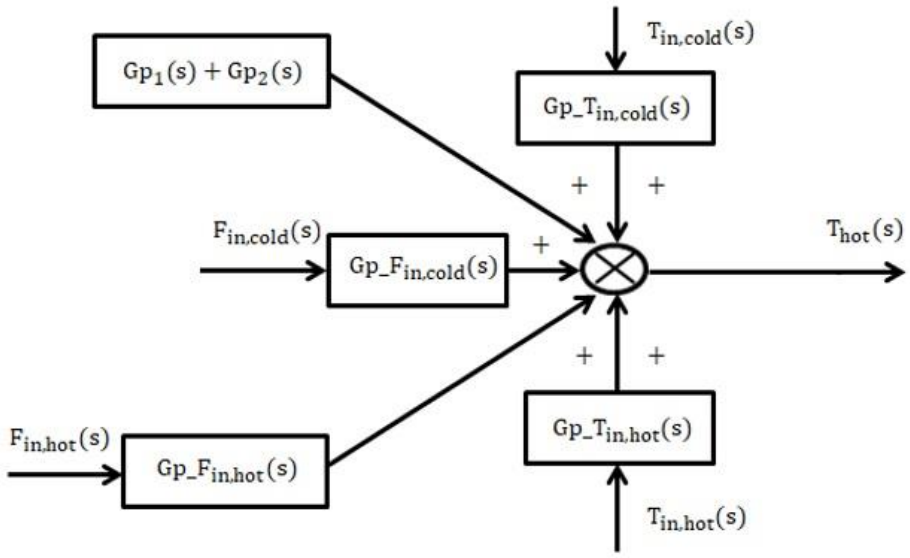

Figure 2.2: Graphical Representation of the Input-Output Relationship for the Open-loop System

In the above figure, the complete open-loop system can be observed. Finally, the table below lists the initial values used for all the control strategies, which will be further analyzed in the following chapters.

Table 2.1: Initial values used in the modeling scheme

Description	**Symbol**	**Value and Units**
Volume of cold side of the exchanger	V_{cold}	0.06 m^3
Volume of hot side of the exchanger	V_{hot}	60 m^3
Tube Area	A	0.06 m^2
Heat transfer coefficient	U	835 $W/m^2 \cdot K$
Inlet flow rate of the cold fluid	Fin_cold	$2.81 \cdot 10^{-5}$ m^3/s
Inlet flow rate of the hot fluid	Fin_hot	0.062 m^3/s
Inlet temperature of the hot fluid	Tin_hot	423 K
Inlet temperature of the cold fluid	Tin_cold	298 K
Density of the cold fluid	ρ_{cold}	1000 kg/m^3
Density of the hot fluid	ρ_{hot}	0.9 kg/m^3
Specific heat of the cold fluid	cp_{cold}	$4.52 \cdot 10^3$ $J/K \cdot kg$
Specific heat of the hot fluid	cp_{hot}	$1.06 \cdot 10^3$ $J/K \cdot kg$
Temperature of the cold fluid at the steady-state point	Tcold_s	320 K
Temperature of the hot fluid at the steady-state point	Thot_s	375.75 K
Flow rate of the cold fluid at the steady-state point	Fin_cold_s	$2.81 \cdot 10^{-5}$ m^3/s

Flow rate of the hot fluid at the steady-state point	Fin_hot_s	0.062 m^3/s
Temperature of the cold fluid at the steady-state point	Tin_cold_s	298 K
Temperature of the hot fluid at the steady-state point	Tin_hot_s	423 K
Temperature of the hot fluid for t=0	T_hot_zero	423 K
Temperature of the cold fluid for t=0	T_cold_zero	298 K

Chapter 3

Control System Set-Up

In this chapter, a theoretical background offering useful information on the fundamentals of control systems will be presented. [18] and [19]. The methodologies that will be used for this purpose include the root locus method for controller tuning, the Ziegler–Nichols and Tyreus-Luyben approaches that adjusts the parameters K_c, t_I, and t_D for the three types of controllers (P, PI, and PID), the model-based or Morari-Zafiriou controller design.

3.1 Description of a Control System

A feedback or feedforward control system can be built through mathematical equations, as presented in Chapter 2 for the shell-and-tube heat exchanger system. A clear method of representing the characteristics of a group of components that form this control system is through block diagrams. These diagrams display input and output signals for each component. That is, one part of the system may receive an input signal and then generate an output signal for another part of the system. There are various forms of signals in engineering applications, such as temperature, fluid flow, pressure, etc.

The block diagram is a simplified and comprehensive way of representing physical systems. Through its use, multiple input or output signals can be identified, as well as the manner in which they are interconnected with the various physical components that make up a control system. Each block in the diagram represents a physical element of the system and is depicted as a rectangular box. Within this box, the transfer function of each block is indicated. Furthermore, a block diagram includes straight lines that symbolize the direction of input and output signals with arrows. Furthermore, each transfer function describes the input and output of a block and is denoted as G(s) and are used in linear models as the ratio of the Laplace transformation of the output variable to the Laplace transformation of the input variable: $G_{(s)} = \frac{Y_{(s)}}{X_{(s)}}$. Essentially, each transfer function represents the input-output relationship and does not provide any additional information about the system's physical behavior. The derivation of transfer functions stems from the differential equations of the system, which are obtained through mathematical modeling (shown in Chapter 2). A simple representation of the transfer function is as follows:

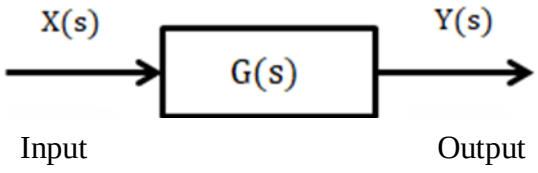

Figure 3.1: A single-input single-output transfer function block

3.2 Description of a Simplified Control System

An automatic control system is defined as the set of physical components that are interconnected in such a way as to guide, control, and regulate the system itself with the aim of operating in a predetermined manner. The control systems that will be discussed below are of the feedback and feedforward type. Before proceeding, the open loop representation will be discussed.

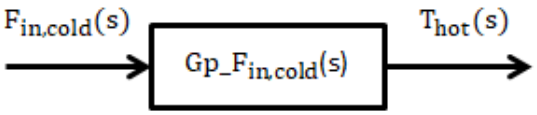

Figure 3.2: Block Diagram of a simplified Open-Loop Control System for a Shell-and-Tube Heat Exchanger

In the above Figure 3.2, the step response diagram of an open-loop control system for the heat exchanger is shown. More specifically, the diagram presents in the Laplace domain the input $F_{in,cold}(s)$, the output $T_{hot}(s)$, and the process transfer function $Gp\_F_{in,cold}(s)$ of the open-loop system (see Chapter 2). The input of the open-loop system represents the flow rate of the cold stream entering the heat exchanger. The output represents the system's response, which is the outlet temperature of the hot stream in the heat exchanger. The process transfer function essentially describes the relationship between the input and output of the open-loop control system.

3.2.1 Closed-Loop Control System

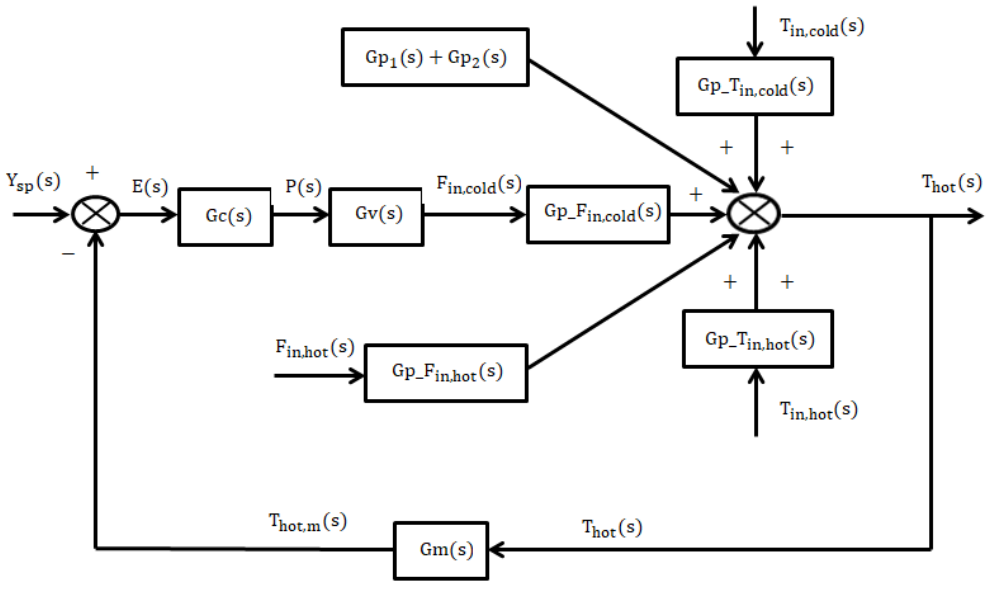

Figure 3.3: Block Diagram of a Closed-Loop Control System for a Shell-and-Tube Heat Exchanger

In the above Figure 3.3, the complete block diagram of a closed-loop control system for a shell-and-tube heat exchanger is presented in the Laplace domain. This approach is based on the authors of sources [13], [16], and [5]. A closed-loop control system is defined as one in which variations in the output $T_{hot}(s)$ directly affect the variations of the inputs $F_{in,hot}(s)$ and $F_{in,cold}(s)$. This type of system is also known as a feedback system. According to sources [20] and [21], the concept of feedback refers to the path of the measured signal of the output variable $T_{hot,m}(s)$ toward the desired input $Y_{sp}(s)$. The purpose of a feedback system is the repeated adjustment of the input variables to eliminate the various disturbances affecting the system. More specifically, the system includes two disturbances, $T_{in,cold}(s)$ and $T_{in,hot}(s)$. The first disturbance is the inlet temperature of the cold flow into the heat exchanger, while the second is the inlet temperature of the hot flow into the heat exchanger, each with their respective transfer functions $Gp\_T_{in,cold}(s)$, $Gp\_T_{in,hot}(s)$:

$$Gp\_T_{in,cold}(s) = \frac{4.099 \cdot 10^{-7}}{(s + 0.0019) \cdot (s + 6.5307 \cdot 10^{-4}) - 1.6169 \cdot 10^{-7}} \qquad (3.1)$$

$$Gp\_T_{in,hot}(s) = \frac{0.001 \cdot s + 6.7484 \cdot 10^{-7}}{(s + 0.0019) \cdot (s + 6.5307 \cdot 10^{-4}) - 1.6169 \cdot 10^{-7}} \qquad (3.2)$$

If these inlet temperatures vary, they affect the system. To prevent this, a transfer function of a measuring element Gm(s) is introduced:

$$Gm(s) = \frac{1}{100 \cdot s + 1} \qquad (3.3)$$

which takes as input the outlet temperature of the hot stream from the heat exchanger $T_{hot}(s)$ and outputs the measured value $T_{hot,m}(s)$. As a physical quantity, the measuring element's transfer function can be a thermocouple. This measured temperature is then compared to the desired reference signal $Y_{sp}(s)$,i.e., which is the desired temperature. This comparison occurs at the input of the controller transfer function Gc(s), where the error is calculated $E(s) = Y_{sp}(s) - T_{hot,m}(s)$. If there is a deviation, the controller sends a command signal P(s) to correct it appropriately. The receiver of this signal is the transfer function of the final control element Gv(s):

$$Gv(s) = \frac{1}{30 \cdot s + 1} \qquad (3.4)$$

which then acts accordingly through an output signal $F_{in,cold}(s)$. Essentially, the final control element is the means by which the controller acts on the system. Physically, this final control element is a valve, through which the controller adjusts the flow rate of the cold stream entering the heat exchanger. This is followed by the process transfer function $Gp\_F_{in,cold}(s)$:

$$Gp\_F_{in,cold}(s) = -\frac{0.3209}{(s + 0.0019) \cdot (s + 6.5307 \cdot 10^{-4}) - 1.6169 \cdot 10^{-7}} \qquad (3.5)$$

which takes as input the change in flow rate of the cold stream, influencing the system's response. The process transfer function is crucial for the heat exchanger, as it enables the required change in the outlet temperature $T_{hot}(s)$ by adjusting the cold stream flow rate. The only input variable that the controller can automatically manipulate is $F_{in,cold}(s)$, because it lies within the closed loop. Based on this correction made by the controller, the hot flow's response will "reach" the same temperature as the reference signal after a period of time and based on the performance of the controller. In addition to the cold flow inlet, there is also a hot flow inlet $F_{in,hot}(s)$ with its corresponding transfer function $Gp\_F_{in,hot}(s)$:

$$Gp\_F_{in,hot}(s) = \frac{0.7875 \cdot s + 5.1429 \cdot 10^{-4}}{(s + 0.0019) * \left(s + 6.5307 \cdot 10^{-4}\right) - 1.6169 \cdot 10^{-7}} \qquad (3.6)$$

As shown in Figure 3.3, the closed-loop response is influenced by multiple transfer functions, $Gp\_T_{in,hot}(s)$, $Gp\_T_{in,cold}(s)$, $Gp\_F_{in,hot}(s)$, $Gp\_F_{in,cold}(s)$. The transfer functions (Gp_1(s) + Gp_2(s)) are required during initialization at t=0:

$$Gp\_1(s) = \frac{47.25 \cdot s + 0.0309}{(s + 0.0019) \cdot \left(s + 6.5307 \cdot 10^{-4}\right) - 1.6169 \cdot 10^{-7}} \qquad (3.7)$$

$$Gp\_2(s) = -\frac{0.0193}{(s + 0.0019) \cdot \left(s + 6.5307 \cdot 10^{-4}\right) - 1.6169 \cdot 10^{-7}} \qquad (3.8)$$

Finally, the shell-and-tube heat exchanger, as a physical system, corresponds to all the transfer functions of the closed-loop system, except for Gv(s), Gc(s), and Gm(s).

The response of the outlet temperature of the hot stream for the closed-loop system in the Laplace domain, including the deviation variables, is calculated using the following formula:

$$T_{hot}'(s) = \frac{Gp\_F_{in,cold}(s) \cdot Gv(s) \cdot Gc(s)}{1 + Gp\_F_{in,cold}(s) \cdot Gv(s) \cdot Gc(s) \cdot Gm(s)} \cdot Y_{sp}'(s) + \frac{Gp\_T_{in,cold}(s)}{1 + Gp\_F_{in,cold}(s) \cdot Gv(s) \cdot Gc(s) \cdot Gm(s)} \cdot T_{in,cold}'(s) + \frac{Gp\_F_{in,hot}(s)}{1 + Gp\_F_{in,cold}(s) \cdot Gv(s) \cdot Gc(s) \cdot Gm(s)} \cdot F_{in,hot}'(s) + \frac{Gp\_T_{in,hot}(s)}{1 + Gp\_F_{in,cold}(s) \cdot Gv(s) \cdot Gc(s) \cdot Gm(s)} \cdot T_{in,hot}'(s) + \frac{Gp_1(s) + Gp_2(s)}{1 + Gp\_F_{in,cold}(s) \cdot Gv(s) \cdot Gc(s) \cdot Gm(s)} \qquad (3.9)$$

The analytical expression for each transfer function is shown in Equation (2.28). The numerator of each fraction is the product of all the transfer functions located between the input signals e.g., $Y_{sp}'(s)$, $T_{in,hot}'(s)$, $F_{in,hot}'(s)$ etc. and the output signal $T_{hot}'(s)$. As for the denominator, which is also the characteristic equation, it results from the product of all the transfer functions within the closed loop i.e., $Gp\_F_{in,cold}(s)$, $Gv(s)$, $Gc(s)$, $Gm(s)$.The addition that appears in the denominator of each fraction arises due to the negative feedback, as shown in Figure 3.3. Finally, the reference signal $Y_{sp}'(s)$, the disturbances $T_{in,hot}'(s)$, $T_{in,cold}'(s)$ and the system input $F_{in,hot}(s)$ can either be constant or varying signals, in the Laplace domain or in time. In each case, they affect the system response.

For the correct design of the controller's transfer function Gc(s), the following conditions must simultaneously be met:

- Stability of both open-loop and closed-loop systems
- The error must be zero, $e = Y_{sp} - T_{hot,m} = 0$
- The system response must "reach" the reference signal quickly

3.3 Root Locus

The root locus is a graphical method developed by Walter Richard Evans in 1948 that determines the poles of the closed-loop transfer function in the Laplace domain. The horizontal axis represents the real part of the poles, while the vertical axis represents the imaginary part. Within these axes, the poles or roots of the characteristic equation move in the closed-loop system, as a system parameter, typically the gain constant K_c varies. This graphical method provides useful information about the system, such as whether it is stable. For the system to be stable, the roots of the characteristic equation must lie to the left of the imaginary axis. If they lie on the vertical axis, the system is marginally stable, while if they lie to the right, the system is characterized as unstable.

Before plotting the root locus, it is necessary to find the roots of the characteristic equation. Essentially, its form arises from the closed-loop system response (3.9), by taking the denominator without the unity term that appears due to negative feedback. In other words, the relationship is as follows:

$$G(s) = Gp\_F_{in,cold}(s) \cdot Gv(s) \cdot Gc(s) \cdot Gm(s) \qquad (3.10)$$

The transfer functions of the final control element and the measuring element are assumed to have a value of one, while the transfer function of the controller corresponds to a proportional controller with a gain constant K_c also equal to one. Therefore, the previous equation transforms into:

$$G(s) = Gp\_F_{in,cold}(s) \qquad (3.11)$$

3.4 Tuning for P, PI and PID Controllers

This section will present the design of three types of controllers P, PI, and PID as well as the parameters that define them (K_c, t_I and t_D) according to sources [17] and [19]. Subsequently, the Ziegler–Nichols method will be employed to achieve tuning of the parameters. This will be carried out using the approximate table provided by the Ziegler–Nichols methodology.

3.4.1 Proportional (P) Controller

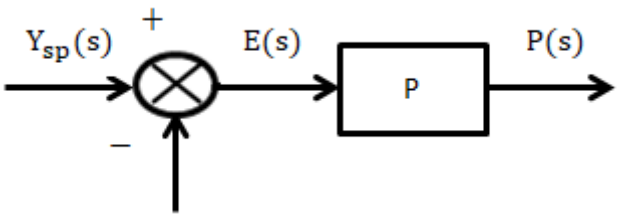

Figure 3.4: Proportional Controller

In the Figure above, a P controller is depicted, and is characterized by a simple construction, hence it has a low cost. The parameter that adjusts a proportional controller is the proportional gain, denoted by K_c. If an appropriate value is assigned to the parameter K_c, any oscillatory behavior in the response of the closed-loop system will be eliminated, resulting in stabilization. Furthermore, the proportional controller with the parameter K_c is quite fast. That is, it acts quickly to bring the system's response back close to the reference signal after possible disturbances. The equation that connects the output and the input of the P controller in the time domain is as follows:

$$P(t) = K_c \cdot E(t) \qquad (3.12)$$

If a Laplace transformation is applied to the previous equation, it results in:

$$P(s) = K_c \cdot E(s) \qquad (3.13)$$

A major drawback of this type of controller is that the response of the closed-loop system cannot exactly "reach" the set point, no matter how much the parameter K_c is adjusted. As a result, there will always be an error (unless stated otherwise).

3.4.2 Proportional–Integral (PI) Controller

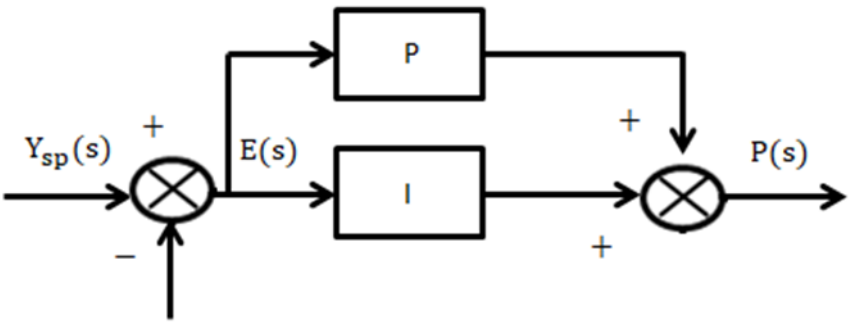

Figure 3.5: Proportional-Integral Controller

In Figure 3.5, the PI controller is presented, which is a more complex controller compared to the proportional or P controller. This type of controller is considered

complex because it requires two parameters to be properly tuned. These parameters are the proportional gain, denoted by K_c, and the integral time constant, denoted by t_I. The advantages this controller has are that it can eliminate the steady-state error due to the presence of the t_I parameter, and it is also quite fast, thanks to the K_c parameter. The equation that connects the output and the input of the PI controller is as follows:

$$P(t) = K_c \cdot E(t) \cdot \left(\frac{K_c}{\tau_I}\right) \cdot \int E(t) \qquad (3.14)$$

If a Laplace transform is applied to the previous equation, it results in:

$$P(s) = K_c \cdot \left[1 + \frac{1}{\tau_I \cdot s}\right] \cdot E(s) \qquad (3.15)$$

The only drawback of this controller is that if the order of the system increases, there is a possibility that the PI controller may introduce instability into the system. This is due to the addition of the second parameter, t_I.

3.4.3 Proportional–Integral-Derivative (PID) Controller

In the above Figure, the PID controller is shown, which is the most complex type of controller, as it requires the tuning of three parameters. The first parameter is the proportional gain, denoted by K_c, the integral time constant, denoted by t_I and the derivative time constant, denoted by, t_D. This type of controller is the most widely used and has a broad range of applications (e.g., production systems, industrial processes). The advantages it offers are zero steady-state error due to the inclusion of the t_I parameter, fast response thanks to the K_c parameter, and reactiveness to sudden changes in the output variable of the closed-loop system because of the t_D parameter. The equation that relates to the output and the input of the PID controller is as follows:

$$P(t) = K_c \cdot E(t) + \left(\frac{K_c}{\tau_I}\right) \cdot \int E(t) + (K_c \cdot \tau_D) \cdot \frac{dE(t)}{dt} \qquad (3.16)$$

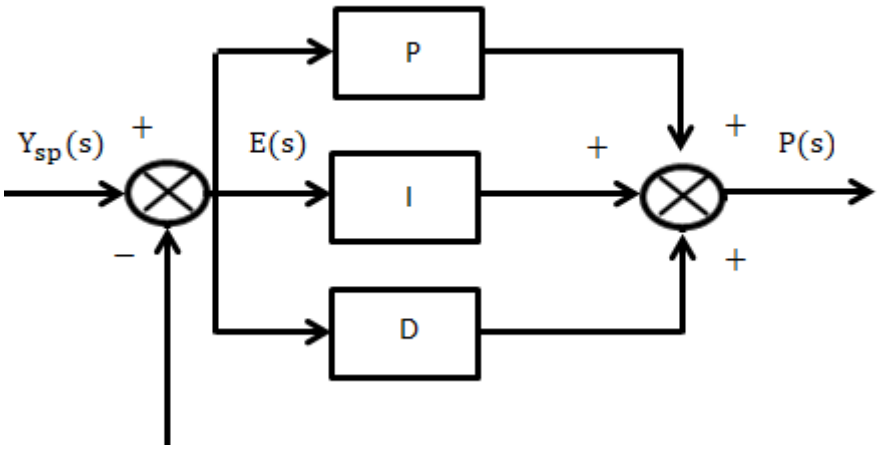

Figure 3.6: Proportional-Integral-Derivative Controller

If a Laplace transform is applied to the previous equation, it results in:

$$P(s) = K_c \cdot \left[1 + \frac{1}{\tau_I \cdot s} + \tau_D \cdot s\right] \cdot E(s) \qquad (3.17)$$

Overall, the PID controller outperforms the other types of controllers. The only challenge is tuning the three parameters K_c, t_I and t_D properly to ensure the controller operates correctly. Below is a table presenting the transfer functions of the three controllers discussed.

Table 3.1: Transfer Functions for the Three Types of Controllers

Types of Controllers	$\mathbf{G_c}$
P Controller	K_c
PI Controller	$K_c \cdot \left(1 + \left(\frac{1}{\tau_I \cdot s}\right)\right)$
PID Controller	$K_c \cdot \left(1 + \left(\frac{1}{\tau_I \cdot s}\right) + \tau_D \cdot s\right)$

3.4.4 The Ziegler-Nichols and Tyreus-Luyben Tuning Methodologies

As its name suggests, the Ziegler–Nichols method was proposed in 1942 by Ziegler and Nichols. This method applies to stable systems and aims to determine suitable values for the parameters K_c, t_I and t_D, so that the three types of controllers (P, PI, PID) can be properly tuned and function correctly in a closed-loop system. Suitable controllers are those that respond effectively to various system disturbances, guiding the system response to "reach" the set point, whether it is constant or time-varying, thereby minimizing or eliminating the system error. To find the values of the parameters K_c, t_I and t_D, a proportional controller must first be applied to the closed-loop system in order to determine the critical gain K_{cr}. Then, the system response should exhibit a continuous oscillatory behavior, allowing the calculation of the critical oscillation period P_{cr}. Once these values are known, the parameters for the three types of controllers can be estimated using the empirical Ziegler–Nichols tuning table. These parameter values were derived from practical experience with manual controller tuning by the two researchers. Thus, they formulated the following empirical, according to source [17]:

Table 3.2: Ziegler-Nichols Table of Parameters

Types of Controllers	K_c	τ_I	τ_D
P Controller	$0.5 \cdot K_{cr}$	–	–
PI Controller	$0.45 \cdot K_{cr}$	$\frac{1}{1.2} \cdot P_{cr}$	–
PID Controller	$0.6 \cdot K_{cr}$	$0.5 \cdot P_{cr}$	$0.125 \cdot P_{cr}$

Following in their footsteps Tyreus and Luyben developed their own tuning table for PI and PID controllers as follows:

Table 3.3: Tyreus-Luyben Table of Parameters

Types of Controllers	K_c	τ_I	τ_D
PI Controller	$\frac{K_{cr}}{3.2}$	$2.2 \cdot P_{cr}$	–
PID Controller	$\frac{K_{cr}}{3.2}$	$2.2 \cdot P_{cr}$	$\frac{P_{cr}}{6.3}$

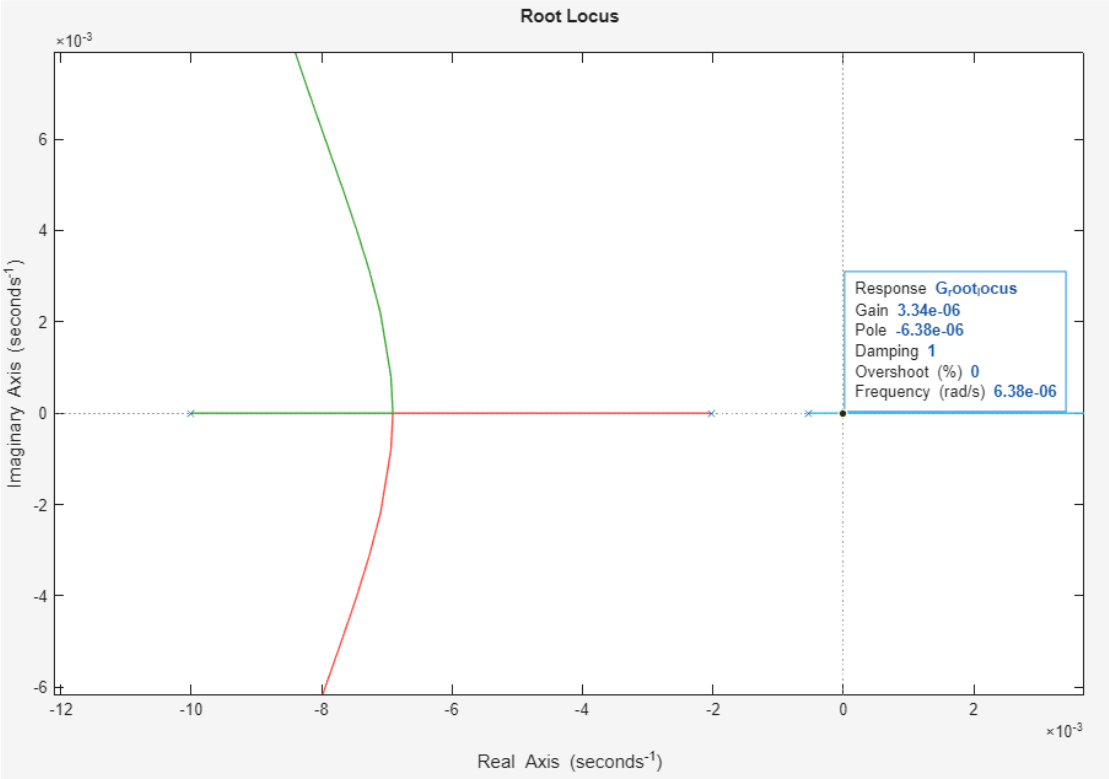

Figure 3.7: Point of marginal stability for the closed-loop system

The above figure is the outcome of the code run onto MATLAB using the Root Locus method. Figure 3.7 holds great value since we can determine the values of critical gain value (Kcr) and critical period of sustained oscillation (Pcr) from it. The point on (0,0)

on the figure corresponds to the point of marginal stability. The information visible on that point translate to:

- Gain is the value of Kcr
- Frequency ω which is the value of the imaginary part of the Pole value

The value retrieved is Kcr = $3.3 \cdot 10^{-6}$, regarding frequency ω, it can be observed that the Pole value on the point of marginal stability does not contain an imaginary part. That observation affects the computation of Pcr since $P_{cr} = \frac{2 \cdot \pi}{\omega}$. Hens, the value of Pcr has to be estimated since it is critical for the Ziegler-Nichols and Tyreus-Luyben methodologies.

3.5 Controller Design Using the Process Model

In this subsection, the design of a controller based on the transfer function model (Gp') for the shell-and-tube heat exchanger system will be carried out, without necessarily adhering to the form of a P, PI, or PID controller. This design will be based on the process transfer function and the Morari–Zafiriou method, as well as certain additional criteria that must be met. The new controller for the system must satisfy three criteria:

- Stability of the closed-loop system
- Zero steady-state error (e = 0)
- Fast system response

First Criterion

To demonstrate the first criterion, namely the stability of the closed-loop system, equation (3.9) is used in the Laplace domain:

$$T_{hot}'(s) = \frac{Gp\_F_{in,cold}(s) \cdot Gv(s) \cdot Gc(s)}{1 + Gp\_F_{in,cold}(s) \cdot Gv(s) \cdot Gc(s) \cdot Gm(s)} \cdot Y_{sp}'(s) + \frac{Gp\_T_{in,cold}(s)}{1 + Gp\_F_{in,cold}(s) \cdot Gv(s) \cdot Gc(s) \cdot Gm(s)} \cdot T_{in,cold}'(s) + \frac{Gp\_F_{in,hot}(s)}{1 + Gp\_F_{in,cold}(s) \cdot Gv(s) \cdot Gc(s) \cdot Gm(s)} \cdot F_{in,hot}'(s) + \frac{Gp\_T_{in,hot}(s)}{1 + Gp\_F_{in,cold}(s) \cdot Gv(s) \cdot Gc(s) \cdot Gm(s)} \cdot T_{in,hot}'(s) + \frac{Gp_1(s) + Gp_2(s)}{1 + Gp\_F_{in,cold}(s) \cdot Gv(s) \cdot Gc(s) \cdot Gm(s)} \quad (3.9)$$

After performing the operations on equation (3.9), the following result is obtained:

$$T_{hot}'(s) = \frac{Gc(s) \cdot Gv(s)}{1 + Gp_{F_{in,cold}(s)} \cdot Gc(s) \cdot Gv(s) \cdot Gm(s)} \cdot Gp\_F_{in,cold}(s) \cdot Y_{sp}'(s) + \left[\frac{Gp_{Tin,cold}(s) + Gp_{F_{in,cold}(s)} \cdot Gc(s) \cdot Gv(s)}{1 + Gp_{F_{in,cold}(s)} \cdot Gc(s) \cdot Gv(s) \cdot Gm(s)} - \frac{Gc(s) \cdot Gv(s)}{1 + Gp_{F_{in,cold}(s)} \cdot Gc(s) \cdot Gv(s) \cdot Gm(s)} \cdot Gp_{F_{in,cold}(s)} \right] \cdot T_{in,cold}'(s) + \left[\frac{Gp_{Fin,hot}(s) + Gp_{F_{in,cold}(s)} \cdot Gc(s) \cdot Gv(s)}{1 + Gp_{F_{in,cold}(s)} \cdot Gc(s) \cdot Gv(s) \cdot Gm(s)} - \frac{Gc(s) \cdot Gv(s)}{1 + Gp_{F_{in,cold}(s)} \cdot Gc(s) \cdot Gv(s) \cdot Gm(s)} \cdot \right.$$

$$Gp_{F_{in,cold}(s)}\Big] \cdot F_{in,\acute{hot}}(s) + \left[\frac{Gp_{Tin},hot(s)+Gp_{F_{in,cold}(s)}\cdot Gc(s)\cdot Gv(s)}{1+Gp_{F_{in,cold}(s)}\cdot Gc(s)\cdot Gv(s)\cdot Gm(s)} - \right.$$

$$\left.\frac{Gc(s)\cdot Gv(s)}{1+Gp_{F_{in,cold}(s)}\cdot Gc(s)\cdot Gv(s)\cdot Gm(s)} \cdot Gp_{F_{in,cold}(s)}\right] \cdot T_{in,\acute{hot}}(s) +$$

$$\left[\frac{Gp_1(s)+Gp_2(s)+Gp_{F_{in,cold}(s)}\cdot Gc(s)\cdot Gv(s)}{1+Gp_{F_{in,cold}(s)}\cdot Gc(s)\cdot Gv(s)\cdot Gm(s)} - \frac{Gc(s)\cdot Gv(s)}{1+Gp\_F_{in,cold}(s)\cdot Gc(s)\cdot Gv(s)\cdot Gm(s)} \cdot Gp\_F_{in,cold}(s)\right]$$

(3.18)

For the first criterion to be satisfied, the following condition must hold:

$$Q(s) = \frac{Gc(s)\cdot Gv(s)}{1+Gp\_Fin,cold(s)\cdot Gc(s)\cdot Gv(s)\cdot Gm(s)} \qquad (3.19)$$

Where Q is any stable transfer function.

From equations (3.18) and (3.19), the system response is obtained in the following form:

$$T_{\acute{hot}}(s) = Q(s)\cdot Gp_{F_{in,cold}(s)}\cdot Y_{\acute{sp}}(s) + \left[\frac{Gp_{Tin},cold(s)+Gp_{F_{in,cold}(s)}\cdot Gc(s)\cdot Gv(s)}{1+Gp_{F_{in,cold}(s)}\cdot Gc(s)\cdot Gv(s)\cdot Gm(s)} - Q(s)\cdot \right.$$

$$\left.Gp_{F_{in,cold}(s)}\right] \cdot T_{in,\acute{cold}}(s) + \left[\frac{Gp_{Fin},hot(s)+Gp_{F_{in,cold}(s)}\cdot Gc(s)\cdot Gv(s)}{1+Gp_{F_{in,cold}(s)}\cdot Gc(s)\cdot Gv(s)\cdot Gm(s)} - Q(s)\cdot Gp_{F_{in,cold}(s)}\right] \cdot$$

$$F_{in,\acute{hot}}(s) + \left[\frac{Gp_{Tin},hot(s)+Gp_{F_{in,cold}(s)}\cdot Gc(s)\cdot Gv(s)}{1+Gp_{F_{in,cold}(s)}\cdot Gc(s)\cdot Gv(s)\cdot Gm(s)} - Q(s)\cdot Gp_{F_{in,cold}(s)}\right] \cdot T_{in,\acute{hot}}(s) +$$

$$\left[\frac{Gp_1(s)+Gp_2(s)+Gp_{F_{in,cold}(s)}\cdot Gc(s)\cdot Gv(s)}{1+Gp_{F_{in,cold}(s)}\cdot Gc(s)\cdot Gv(s)\cdot Gm(s)} - Q(s)\cdot Gp_{F_{in,cold}(s)}\right] \quad (3.20)$$

Second Criterion

Next, to satisfy the second criterion, the final value theorem will be used. This theorem describes the behavior of the function f(t) as time approaches infinity. For this theorem to hold, the first derivative of f(t) must be Laplace-transformable, and the denominator of the function s·F(s) must not have roots on the imaginary axis or in the right half of the complex plane.

$$\lim_{t\to\infty} f(t) = \lim_{s\to 0} sF(s) \quad (3.21)$$

The error is defined in the Laplace domain (the tilde corresponds to the deviation variable) as:

$$E(s) = Y_{\acute{sp}}(s) - T_{\acute{hot}}(s) \qquad (3.22)$$

In equation (3.22), a substitution is made where F(s) = E(s), and the limit must approach zero for the second criterion (zero error) to be satisfied.

$$\lim_{s\to 0} sE(s) = \lim_{s\to 0}[s(Y_{sp}'(s) - T_{hot}'(s))] \qquad (3.23)$$

By substituting equation (3.20) into equation (3.23) and explicitly expressing the deviation variables (e.g., $Y_{sp}'(s) = \frac{Y_{sp} - T_{hot,s}}{s}$), after some calculations, the following result is obtained:

$$\lim_{s\to 0} sE(s) = 0 \qquad (3.24)$$

Third Criterion

Furthermore, for the third criterion, that is, the dynamic performance of the system based on the design of the new controller, the process transfer function will be divided into two parts:

$$Gp(s) = Gp^{-}(s) \cdot Gp^{+}(s) \qquad (3.25)$$

The first part, $Gp^{-}(s)$, is called the product of transfer functions that are minimum-phase and essentially reflects the "clean" or desired part. In contrast, the second part, $Gp^{+}(s)$, is the product of transfer functions that are non-minimum-phase and essentially represents the "undesirable" part. This portion may include:

- Dead time (e.g., an exponential term)
- Zeros in the right half of the complex plane (e.g., in the numerator of the transfer function)
- $|Gp^{+}(s = i\omega)| = 1$

In the case of the heat exchanger, the process transfer function is purely minimum phase, that is:

$$Gp(s) = Gp^{-}(s) = Gp\_F_{in,cold}(s) \cdot Gv(s) \cdot Gm(s) \qquad (3.26)$$

In addition, equation (3.11) can be changed to:

$$Gc(s) = \frac{Q(s)}{Gv(s)\cdot[1 - Gp_{Fin,cold(s)}\cdot Gm(s)\cdot Q(s)]} \qquad (3.27)$$

For optimal dynamic performance, the following equation must hold:

$$Q_{min}(s) = \frac{1}{Gp^{-}(s)} \qquad (3.28)$$

If a substitution is made in (3.27), with (3.28) for $Q(s) = Q_{min}(s)$ then:

$$Gc_{,min}(s) = \left(\frac{1}{Gp^{-}(s)}\right) \cdot \left(\frac{1}{1 - Gp^{+}(s)}\right) \qquad (3.29)$$

Summing up, all three criteria for the design of the new controller have now been presented. However, for the third criterion, equation (3.29), there is a possibility that the resulting controller transfer function may take an indeterminate form. Specifically,

this can occur when the degree of the numerator polynomial of Gp(s) is greater than the degree of its denominator. This issue may arise either if the controller transfer function is purely minimum phase or if it is a combination of minimum and non-minimum phase with the presence of positive zeros. To address this problem, the Morari–Zafiriou methodology provides a solution using the following formula:

$$\mathrm{Q(s)} = \frac{1}{(\lambda \cdot \mathrm{s}+1)^{\mathrm{r}}} \cdot \mathrm{Q_{min}(s)} = \frac{1}{(\lambda \cdot \mathrm{s}+1)^{\mathrm{r}}} \cdot \frac{1}{\mathrm{Gp^{-}(s)}} \quad (3.30)$$

By substituting equation (3.30) into equation (3.27), the desired form of the controller transfer function is obtained after performing the necessary calculations:

$$\mathrm{Gc(s)} = \frac{1}{\mathrm{Gp^{-}(s)}} \cdot \frac{1}{(\lambda \cdot \mathrm{s}+1)^{\mathrm{r}} - \mathrm{Gp^{+}(s)}} \quad (3.31)$$

substituting the values the following equation is obtained:

$$\mathrm{Gc(s)} = -\frac{3.1159 \cdot (30 \cdot \mathrm{s}+1) \cdot (100 \cdot \mathrm{s}+1) \cdot \left((\mathrm{s}+0.0019) \cdot (\mathrm{s}+6.5307 \cdot 10^{-4}) - 1.6169 \cdot 10^{-7}\right)}{((\mathrm{s}+1)^4 - 1)} \quad (3.32)$$

The new controller type can be tuned using only one variable, in contrast to PI and PID controllers, which depend on multiple parameters. This single variable is λ, which represents a small time constant. The exponential term r in the new controller formula, equation (3.32), is the difference between the degree of the denominator polynomial and the degree of the numerator polynomial of Gp(s).

As previously mentioned in equation (3.26), the process transfer function is purely minimum phase. Therefore, in order to determine the value of r, the explicit expression of the process transfer function must be formulated, which is as follows:

$$Gp(s) = Gp^{-}(s) = Gp_{Fin,cold}(s) \cdot \mathrm{Gv(s)} \cdot \mathrm{Gm(s)} = \frac{\left[\frac{U \cdot \mathrm{A}}{\rho_{hot} \cdot c_{p,hot} \cdot V_{hot}}\right]_s \cdot \left[\frac{T_{in,cold} - T_{cold}}{V_{cold}}\right]_s}{\left[s + \left(\frac{F_{in,hot}}{V_{hot}} + \frac{U \cdot \mathrm{A}}{\rho_{hot} \cdot c_{p,hot} \cdot V_{hot}}\right)_s\right] \cdot \left[s + \left(\frac{F_{in,cold}}{V_{cold}} + \frac{U \cdot \mathrm{A}}{\rho_{cold} \cdot c_{p,cold} \cdot V_{cold}}\right)_s\right] - \left[\frac{(U \cdot \mathrm{A})^2}{\rho_{hot} \cdot c_{p,hot} \cdot V_{hot} \cdot \rho_{cold} \cdot c_{p,cold} \cdot V_{cold}}\right]_s} \cdot \frac{1}{30 \cdot \mathrm{s}+1} \cdot \frac{1}{100 \cdot \mathrm{s}+1} \quad (3.33)$$

It is observed that it is of fourth order, so:

r = degree of denominator polynomial - degree numerator polynomial = 4 – 0 = 4

The formulas in equations (3.25), (3.27), and (3.28) are also verified by sources [13], [16], and [5].

Chapter 4

Simulations for a Shell-and-tube Heat Exchanger in a feedback loop

In this chapter, an analysis of the closed-loop system results will be conducted for the various types of controllers mentioned in the previous Chapter. The analysis will be carried out for different simulation scenarios and a comparison will be made. More specifically, a comparison between the design using the Ziegler–Nichols methodology, the Tyreus-Luyben methodology and the design using the model-based methodology.

4.1 Corrections for the Tuning tables

The value of P_{cr} has to be estimated due to certain assumptions, which lead the system response to lack sustained oscillatory behavior. Therefore, a code was developed in the MATLAB software, which implements the Ziegler–Nichols methodology and includes the values of the tuning table shown in chapter 3. However, the response and error results for the three types of controllers were not satisfactory, and thus corrective adjustments were made to the Ziegler–Nichols table in order to achieve more reasonable and accurate results.

Table 4.1: Corrected Ziegler-Nichols Table of Parameters (negative due to the effect of the input to the output variable)

Types of Controllers	K_c	τ_I	τ_D
P Controller	$-1.65 \cdot 10^{-5}$	∞	0
PI Controller	$-1.485 \cdot 10^{-5}$	9747.8	0
PID Controller	$-1.98 \cdot 10^{-5}$	5848.7	2088.8

The same phenomenon applies to Tyreus-Luyben, thus corrective adjustments are:

Table 4.2: Corrected Tyreus-Luyben Table of Parameters (negative due to the effect of the input to the output variable)

Types of Controllers	K_c	τ_I	τ_D
PI Controller	$-1.0312 \cdot 10^{-5}$	36763.3	–
PID Controller	$-1.0312 \cdot 10^{-5}$	36763.3	2652.5

Detailed results will be presented, in this chapter, for various simulation scenarios involving the 6 different types of controllers, such as: constant reference signal, changes in the reference signal and changes in system disturbances.

4.2 Simulation and Comparison of the Linear Models

In this specific subsection, the comparative results of the closed-loop system for the linear models will be presented. The simulations will concern:

- A constant reference signal at 375K.
- A variable reference signal (changes will be made arbitrarily)
- A constant reference signal at 375K and the introduction of the disturbances $T_{in,hot}$, $T_{in,cold}$ (changes will be made arbitrarily)

Below a diagram of the constant and variable reference signals is presented:

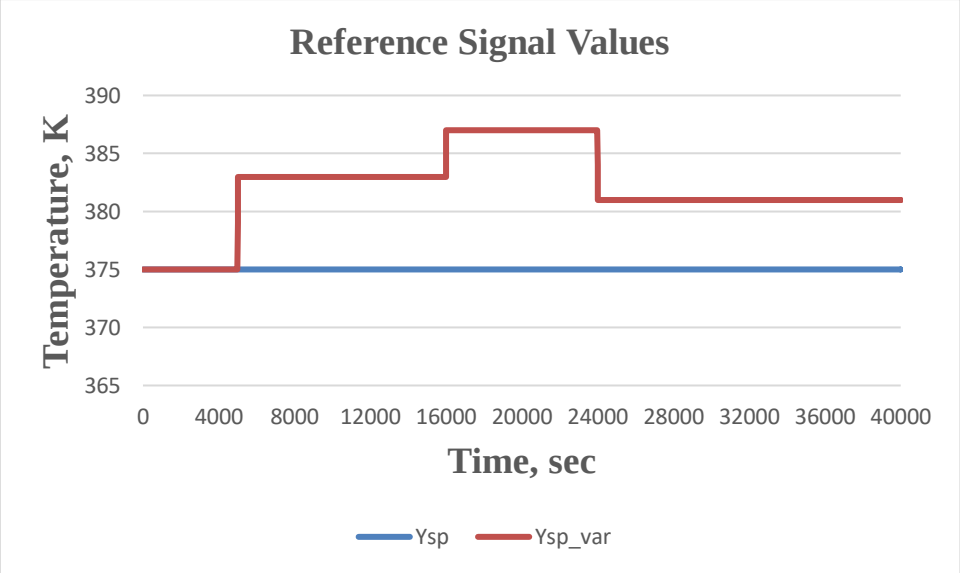

Diagram 4.1: The reference signal values for the closed-loop system

4.2.1 Simulation for Constant Reference Signal

Regarding this simulation, the closed-loop system has a constant reference signal with a temperature value of 375 K and with a simulation time up to 10000 seconds.

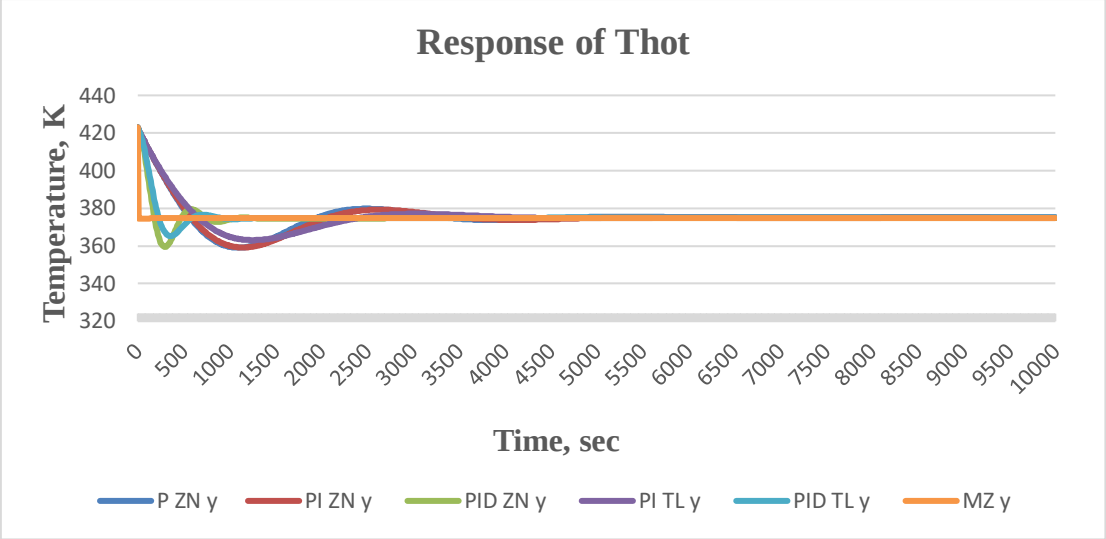

Diagram 4.2: The response of the Thot for the closed-loop system in relation to the different types of controllers

From the above diagram the response of the value Thot of the heat exchanger can be observed in relation to different types of controllers. The simulation runs for 10000 seconds, the starting temperature is 423 K (t=0), and the desired outcome is stabilization at 375 K (constant set-point). The P and PI controllers with the Ziegler-Nichols methodology exhibit the same oscillatory behavior throughout the simulation. They start at 423 K, then there is a small fluctuation in the temperature, and in the end, the temperature reaches the reference signal. The same can be said for the PI controllers with the Tyreus-Luyben methodology, although the fluctuations there were milder in contrast to the Ziegler-Nichols. Furthermore, the PID controllers for both Ziegler-Nichols and Tyreus-Luyben methodologies exhibit the same fluctuation pattern as well. The oscillations stopped faster than on the P and PI controllers and were milder for the Tyreus-Luyben than the Ziegler-Nichols. Lastly there is the Morari-Zafiriou controller, who reaches the predetermined set point instantly with nearly no fluctuation observed.

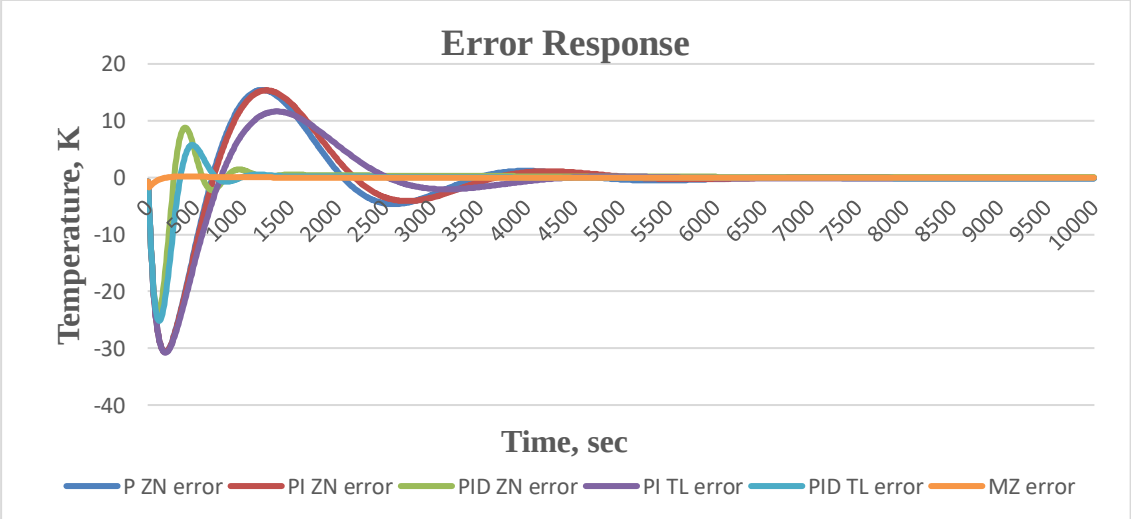

Diagram 4.3: Error exhibited for the closed-loop system in relation to the different types of controllers

In the above diagram, the error (difference between the set-point and the exit variable that needs to be controlled) for the heat exchanger system caused by the various types of controllers is presented. More specifically, the same error behavior apply to the P and PI controllers. That is, fluctuations are observed, just like in the system's response. For Ziegler-Nichols methodology, after 10000 seconds, the P controller results in a small error of about -0.122, while the PI controller achieves a zero error. For Tyreus-Luyben methodology after 10000 seconds, the PI controller shows an error of -0.1057. Similarly, the errors of the PID controllers for Ziegler-Nichols and Tyreus-Luyben methodologies exhibit similar behavior as the P and PI controllers. In contrast though, the error is minimized very quickly in each case. For Ziegler-Nichols after 10000 seconds the error reaches a value of zero. For Tyreus-Luyben the error never truly reaches zero, although it fluctuates between -0.0582 and -0.0997 after 6280 seconds. It truly reaches zero momentarily at 4440 seconds, then it deviates again. Finally, regarding the Morrari-Zafiriou controller it can be observed that it minimizes its error the fastest. It reaches zero momentarily at 2230 then it deviates up to zero at 2990 seconds, after the error starts to decrease again and finally reaches a value of zero at 10000 seconds.

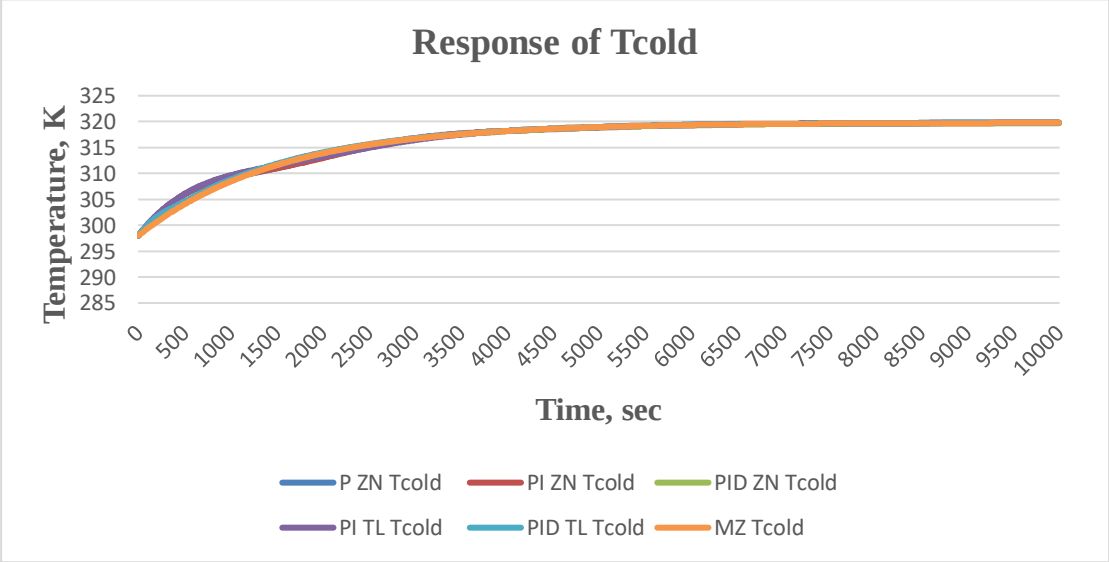

Diagram 4.4: Tcold response for the closed-loop system in relation to the different types of controllers

The above diagram displays the response of the temperature of the cold flow for the heat exchanger, in relation to various types of controllers. It is observed that the response of the cold flow is similar for all the controllers. The cold flow starts at 298 K and increases to 319.8 K after 10000 seconds. Additionally, something worth noting is that P and PI controllers for both Ziegler-Nichols and Tyreus-Luyben methodologies exhibit a slight fluctuation at the start of the simulation, whereas it is not present for the PID and Morrari-Zafiriou controllers.

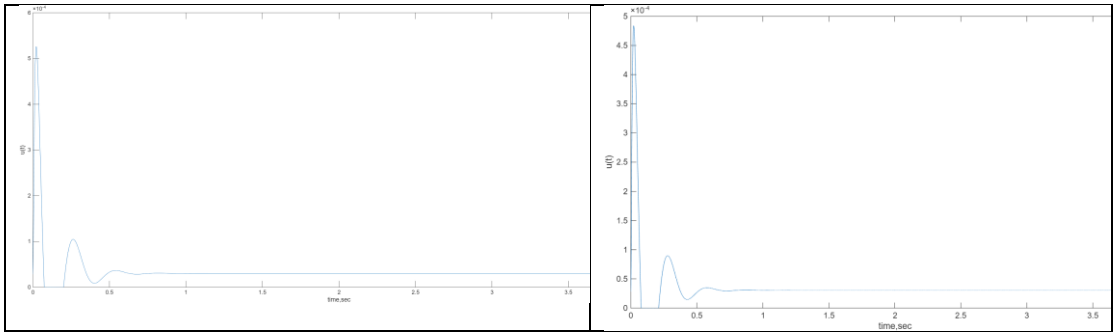

Diagram 4.4a: U(t) for the P controller ZN (left) and PI controller ZN (right)

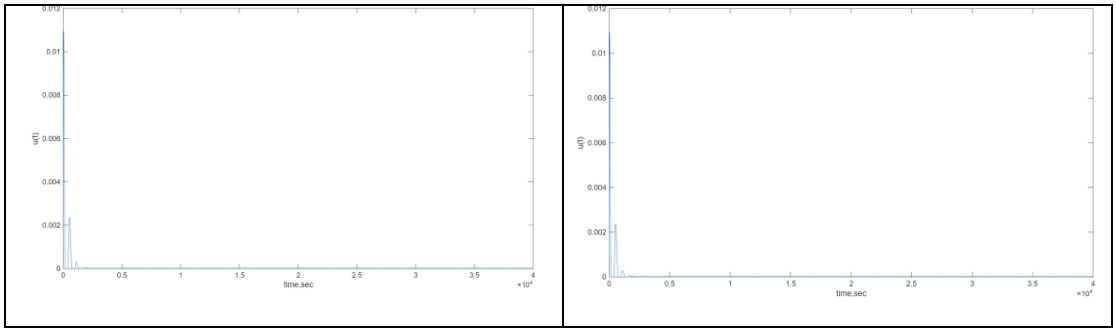

Diagram 4.4b: U(t) for the the PID controller ZN (left) and the PI controller TL (right)

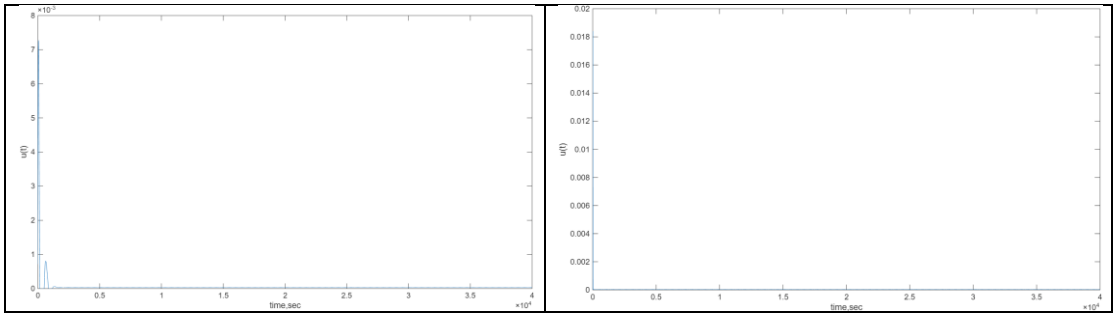

Diagram 4.4c: U(t) for the PID controller TL (left) and Morari-Zafiriou controller (right)

4.2.2 Simulation for Variable Reference Signal

The second simulation consists of a variable reference signal over the course of 40000 seconds. At the start, the reference temperature was 375 K, then it increased at 383 K at 5000 seconds. In addition, it increased again at 16000 seconds to 387 K and finally decreased to 381 at 24000 seconds.

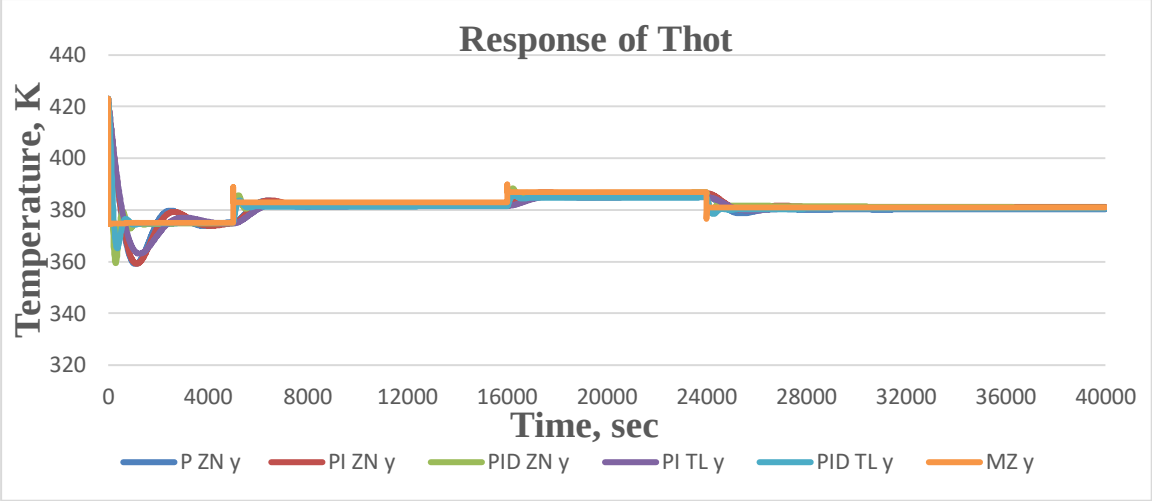

Diagram 4.5: The response of the Thot for the closed-loop system in relation to the different types of controllers

From the above Diagram 4.4, the temperature response of the hot flow in the heat exchanger is observed with respect to different types of controllers. The P controller appears to exhibit the same oscillatory behavior as the PI controller for both Ziegler-Nichols and Tyreus-Luyben, although Tyreus-Luyben shows a smaller oscillation range than Ziegler-Nichols. Additionally, the PID controllers for both methodologies appear to reach the reference signal very fast, with the controller of Tyreus-Luyben again showing a smaller oscillation range. Finally, the Morari–Zafiriou controller tracks the reference signal with high speed without any fluctuations. It is observed that these specific controllers make the necessary corrective actions each time, so that the closed-loop response follows the reference signal throughout any change over time. For all the controllers, even smaller oscillatory behaviors appear in the system response at every change of the reference signal over time. However, in the end, the closed-loop responses do follow the reference signal.

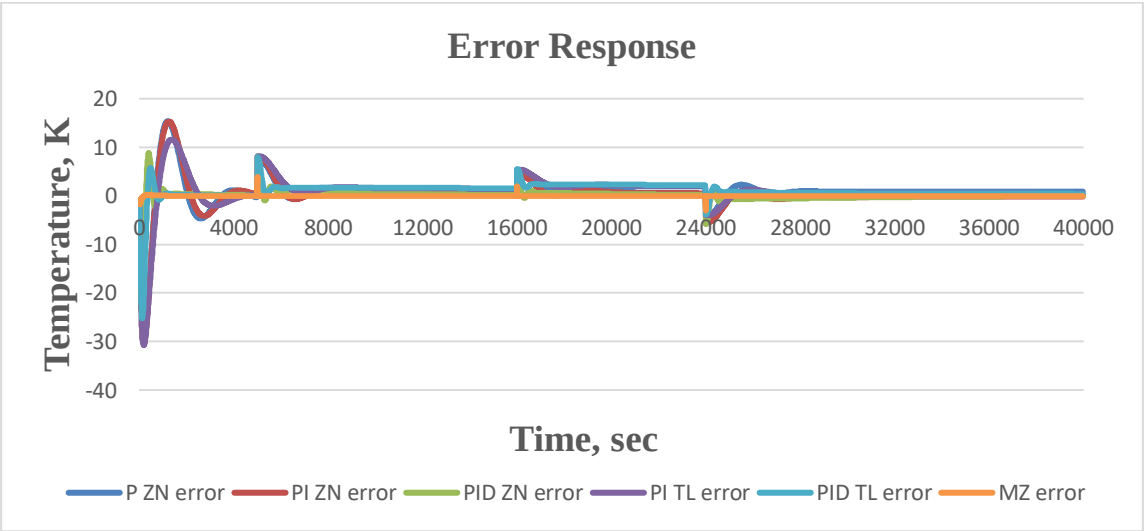

Diagram 4.6: Error exhibited for the closed-loop system in relation to the different types of controllers

In the above Diagram 4.5, the error for the heat exchanger system generated by the various types of controllers is presented. More specifically, the P and PI controllers for both methodologies exhibit fluctuations in the error, just as in the system's response. The same behavior is observed for the PID controllers as well, though the error gets minimized fairly quickly than it did for the P and PI controllers. Then, there is the Morari-Zafiriou controller, that exhibits error only momentarily, at the start of the simulation and when the change at the reference signal occurs. After 40,000 seconds, the P controller of the Ziegler-Nichols methodology results in an error of 0.8926, the PI controller of the Ziegler-Nichols methodology results in an error of -0.0977, the PI controller of the Tyreus-Luyben methodology results in an error of 0.4234. Then the PID controller of the Ziegler-Nichols methodology results in an error of -0.0316 and the PID controller of the Tyreus-Luyben methodology results in an error of 0.4373. Finally, the Morari–Zafiriou controller, regardless of changing reference signal, yields zero error.

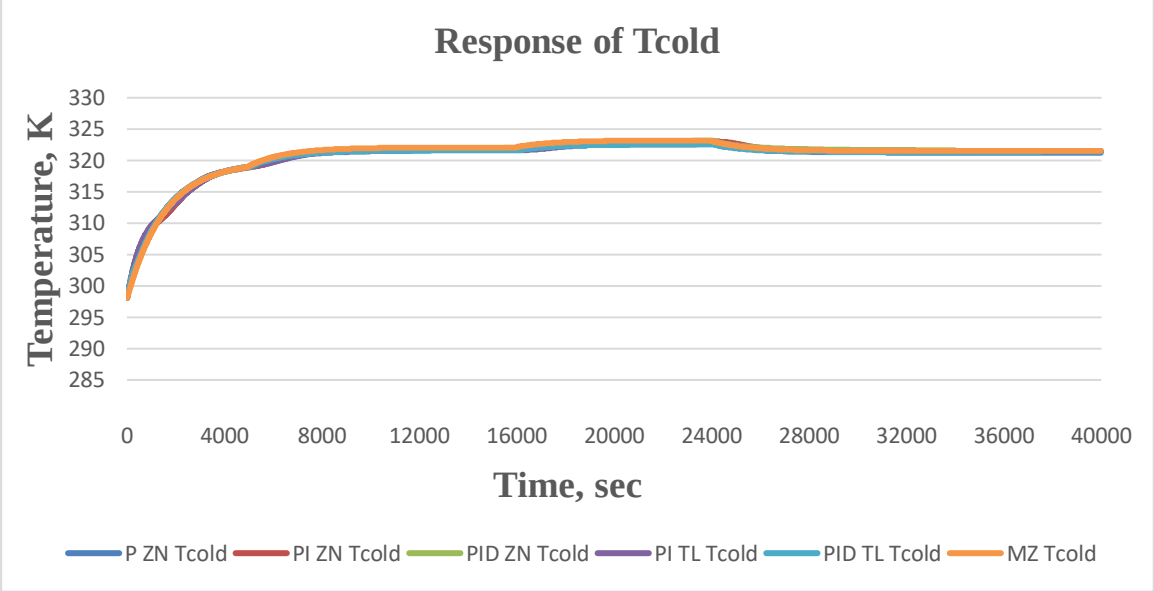

Diagram 4.7: Tcold response for the closed-loop system in relation to the different types of controllers

The diagram above displays the response of the temperature of the cold flow for the heat exchanger, in relation to various types of controllers. It is observed that the response of the cold flow is similar for all the controllers. The increase or decrease of the temperature of the cold flow corresponds to the changes of the reference signal throughout the simulation.

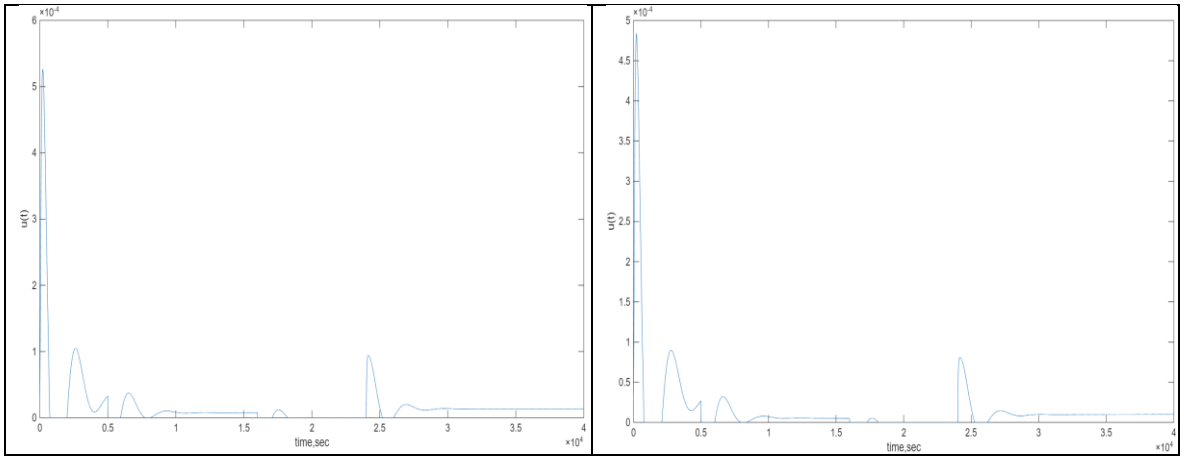

Diagram 4.7a: U(t) for the P controller ZN (left) and PI controller ZN (right)

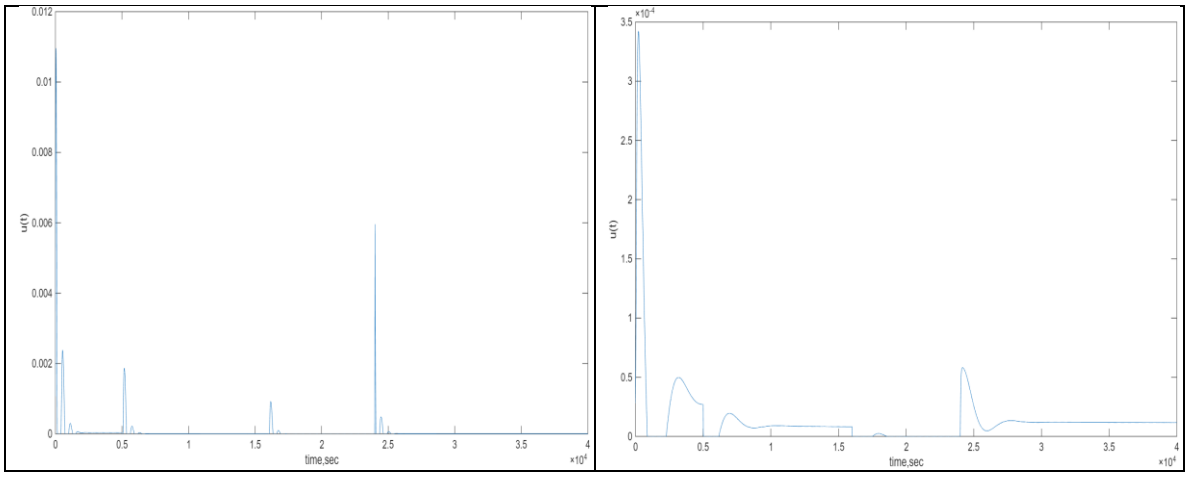

Diagram 4.7b: U(t) for the the PID controller ZN (left) and the PI controller TL (right)

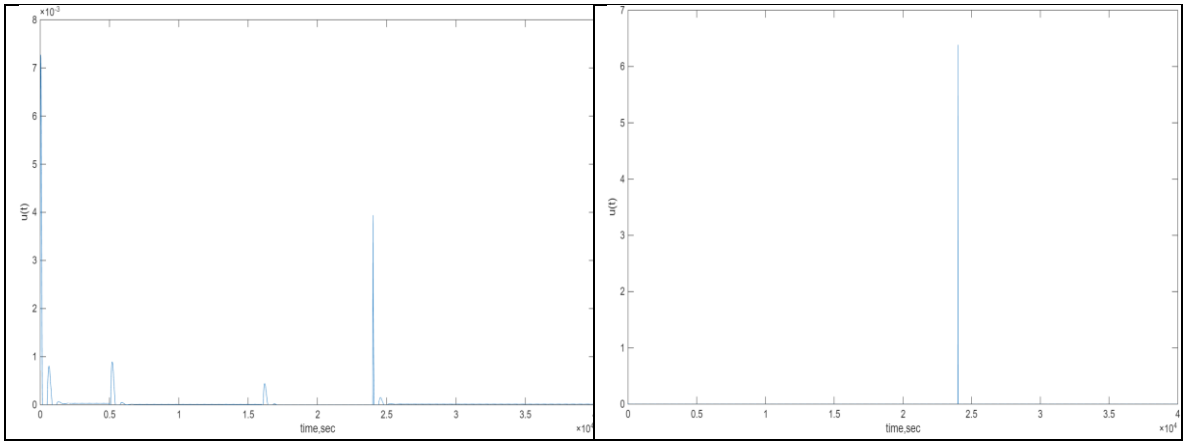

Diagram 4.7c: U(t) for the PID controller TL (left) and Morari-Zafiriou controller (right)

4.2.3 Simulation for a constant reference signal and the introduction of the disturbances $T_{in,hot}$, $T_{in,cold}$

The third simulation consists of a constant reference signal at 375 K and the introduction of two disturbances. The diagram below expresses exactly that:

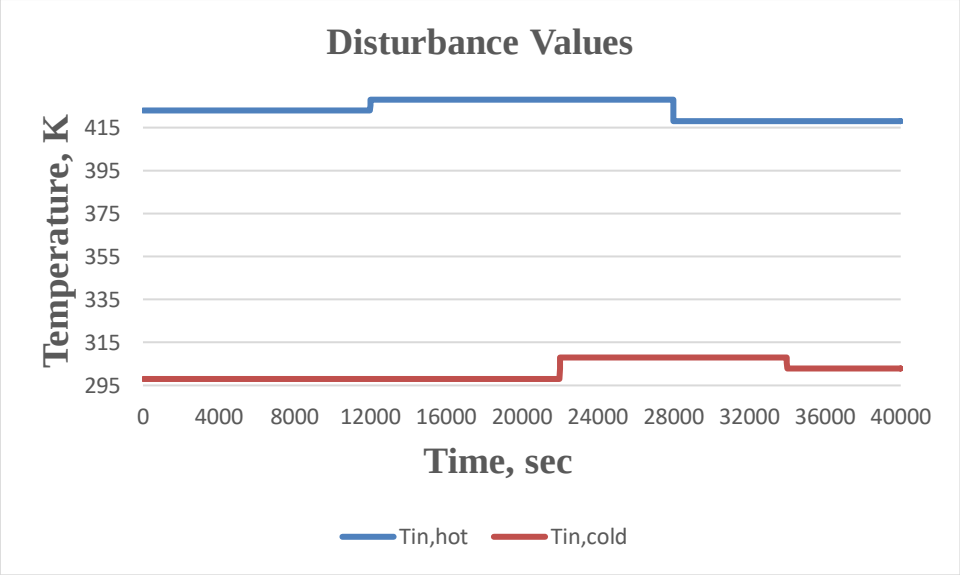

Diagram 4.8: The Disturbance values for the closed-loop system

The inlet temperature of the hot flow $T_{in,hot}$ is the first disturbance. Initially, it has a temperature of 423 K, at 12010 seconds it increases to 428 K and finally decreases to 418 K at 28010 seconds. In addition, the inlet temperature of the cold flow $T_{in,cold}$ is the second disturbance. In the beginning it has a temperature of 298 K, at 22010 seconds it increases to 308 K and finally decreases to 303 K at 34010 seconds.

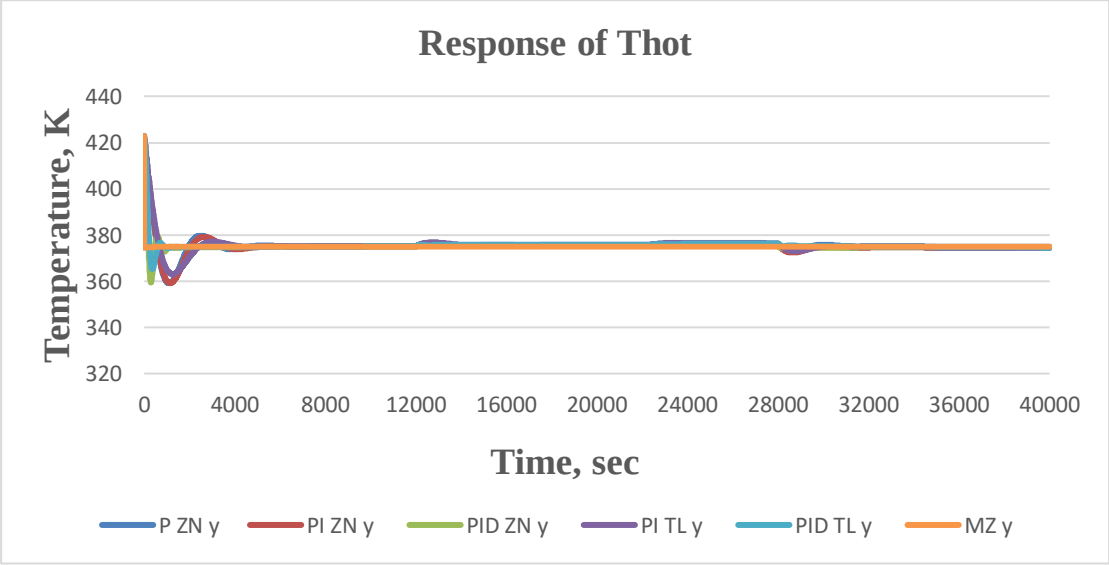

Diagram 4.9: The response of the Thot for the closed-loop system in relation to the different types of controllers

The above diagram 4.7 expresses the response of the output Thot of the closed-loop system in relation to a variety of controllers. It can be observed that the P and PI controllers for but Ziegler-Nichols and Tyreus-Luyben methodologies show a miniscule fluctuation at the start of the simulation, up until 6000 seconds, when they stabilize at the predetermined setpoint of 375 K. Whereas the PID controllers stabilize at the setpoint much faster, with the Morari-Zafiriou instantly catching the reference

signal value. As it seems the disturbance values of $T_{in,hot}$ and $T_{in,cold}$ do not affect the output value of Thot by a lot. The P and PI controllers show a minor oscillation roughly at 29000 Seconds. On the other hand, the PID and Morari-Zafiriou controllers are not affected at all from the disturbances

.

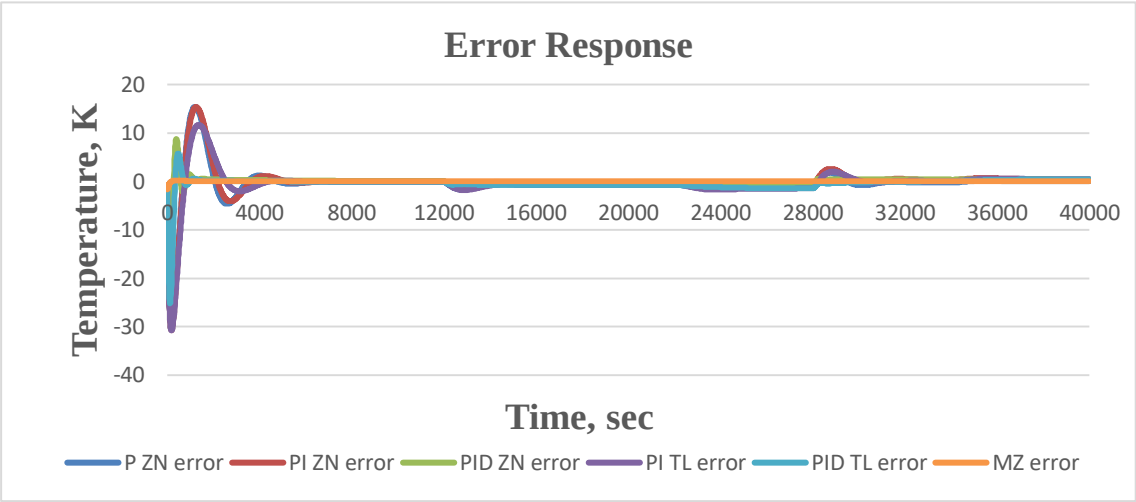

Diagram 4.10: Error exhibited for the closed-loop system in relation to the different types of controllers

The above diagram 4.8 expresses the error response of the closed-loop system in relation to a variety of controllers. The oscillatory behavior of all the controllers is much clearer in this diagram than diagram 4.7. Here, it can be observed that the ones who stabilize at the setpoint value last are the P and PI controllers for both methodologies, with the Tyreus-Luyben PI controller exhibiting a lower peak of oscillation. Also, the effect of the disturbances is present here as well.

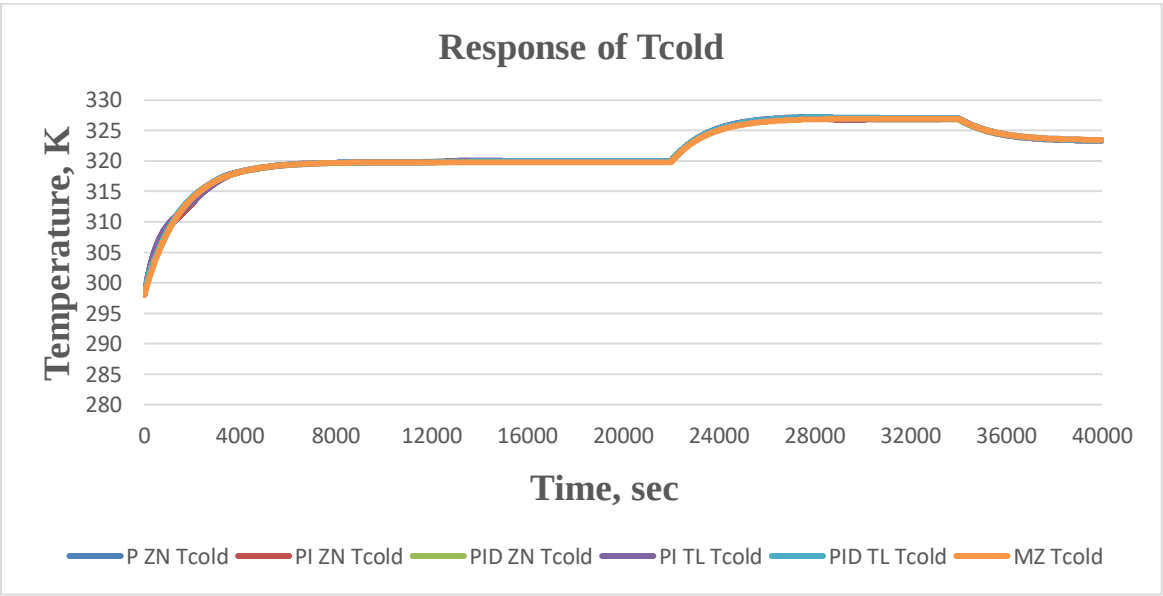

Diagram 4.11: Tcold response for the closed-loop system in relation to the different types of controllers

Lastly in the above diagram 4.9 the response of Tcold is exhibited for all the different types of controllers. It is observed that the Tcold value is nearly identical for all the different controllers. The sudden changes seen in the temperature of Tcold are caused by the disturbances $T_{in,hot}$ and $T_{in,cold}$.

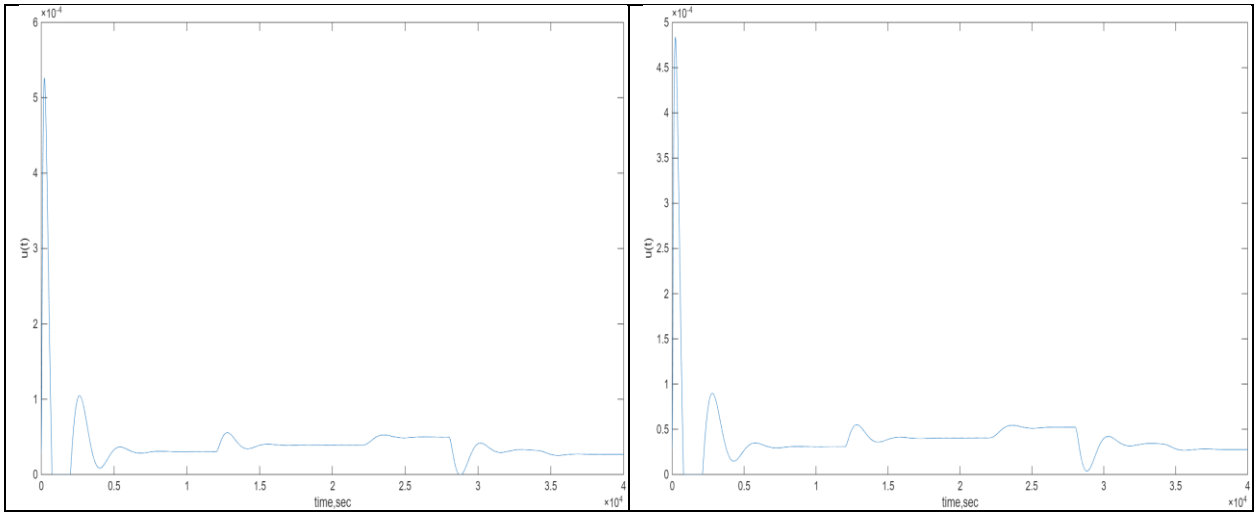

Diagram 4.11a: U(t) for the P controller ZN (left) and PI controller ZN (right)

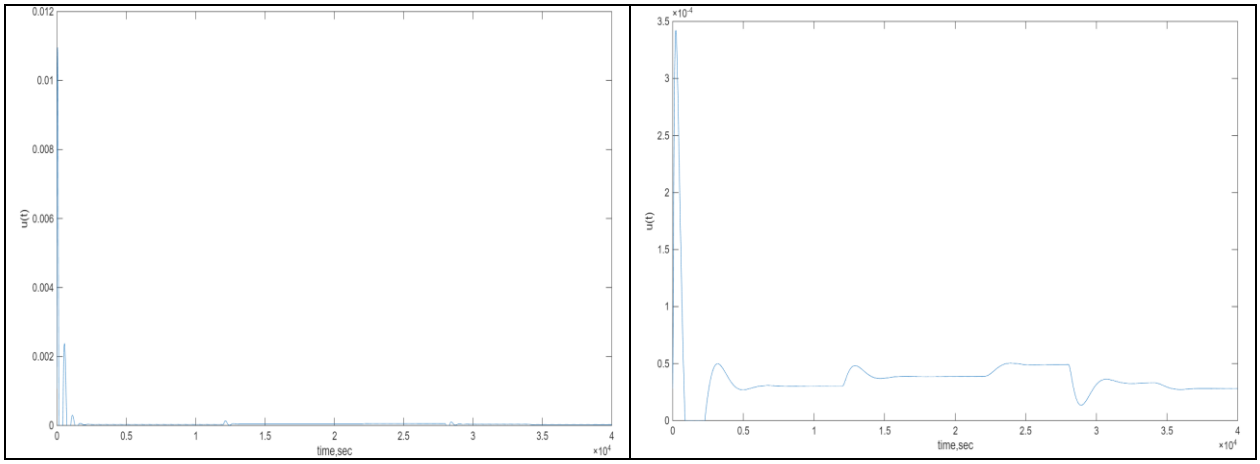

Diagram 4.11b: U(t) for the the PID controller ZN (left) and the PI controller TL (right)

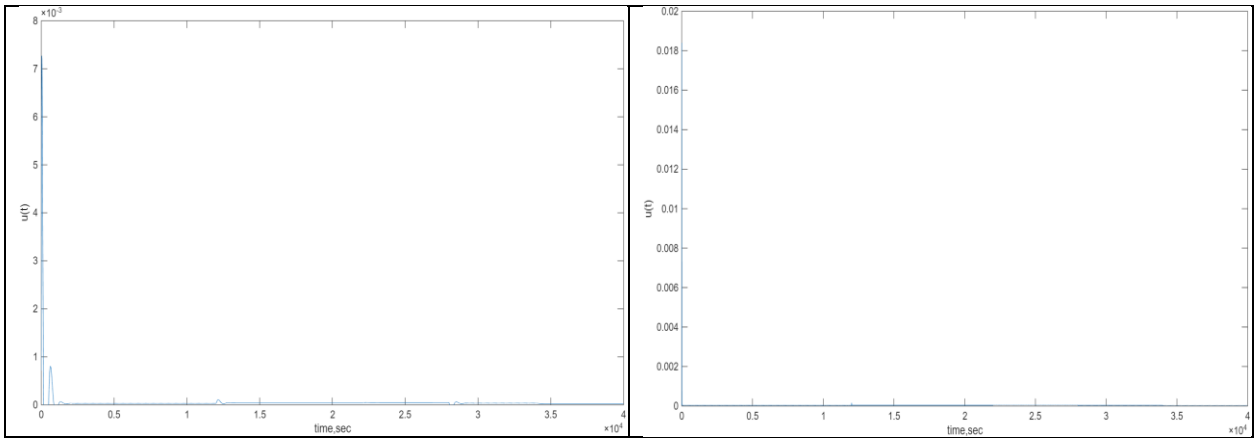

Diagram 4.11c: U(t) for the PID controller TL (left) and Morari-Zafiriou controller (right)

4.2.4 Comparison of the different types of controllers

In this subsection, a variety of performance criteria are used to evaluate the efficiency and effectiveness of the controllers for each simulation scenario.

- **ISE (Integral of Squared Error):**

$$ISE = \int_0^\infty e^2(t)\,dt$$

It emphasizes large error values more heavily. It is useful when penalizing large deviations as a priority.

- **IAE (Integral of Absolute Error):**

$$IAE = \int_0^\infty |\,e(t)\,|\;dt$$

It penalizes the total error value over time equally, regardless of magnitude. It tends to produce smoother control actions.

- **ITSE (Integral of Time-weighted Squared Error):**

$$ITSE = \int_0^\infty t \cdot e^2(t)\,dt$$

Places more weight on error values that persist over time. It helps to reduce long-term error.

- **IATE (Integral of Time-weighted Absolute Error):**

$$IATE = \int_0^\infty t \cdot |\,e(t)\,|\;dt$$

Similar to ITSE but gives linear weight to error values over time, focusing on sustained error reduction.

Table 4.1: Performance Criteria of control for constant reference signal

Performance Criteria	P ZN	PI ZN	PID ZN	PI TL	PID TL	Morari-Zafiriou
ISE	$4.638 \cdot 10^4$	$4.746 \cdot 10^4$	**$8.811 \cdot 10^3$**	$4.258 \cdot 10^4$	$1.072 \cdot 10^4$	**14.3992**
IAE	$3.52 \cdot 10^3$	$3.169 \cdot 10^3$	**815.5096**	$3.091 \cdot 10^3$	985.6262	**26.2201**
ITSE	$3.229 \cdot 10^7$	$3.272 \cdot 10^7$	**$1.543 \cdot 10^6$**	$2.541 \cdot 10^7$	$2.133 \cdot 10^6$	**$1.359 \cdot 10^3$**
IATE	$1.367 \cdot 10^7$	$3.96 \cdot 10^6$	**$9.924 \cdot 10^5$**	$8.916 \cdot 10^6$	$6.232 \cdot 10^6$	**$1.353 \cdot 10^4$**
Utot	0.1420	0.1419	0.2625	0.1324	0.2041	0.1410

Table 4.2: Performance Criteria of control for variable reference signal

Performance Criteria	P ZN	PI ZN	PID ZN	PI TL	PID TL	Morari-Zafiriou
ISE	$5.699 \cdot 10^4$	$5.468 \cdot 10^4$	$\mathbf{1.104 \cdot 10^4}$	$5.599 \cdot 10^4$	$1.981 \cdot 10^4$	**43.4001**
IAE	$8.043 \cdot 10^3$	$5.921 \cdot 10^3$	$\mathbf{2.523 \cdot 10^3}$	$7.993 \cdot 10^3$	$5.479 \cdot 10^3$	**35.4005**
ITSE	$2.04 \cdot 10^8$	$1.251 \cdot 10^8$	$\mathbf{3.045 \cdot 10^7}$	$2.109 \cdot 10^8$	$1.485 \cdot 10^8$	$\mathbf{3.614 \cdot 10^5}$
IATE	$1.036 \cdot 10^8$	$4.914 \cdot 10^7$	$\mathbf{3.051 \cdot 10^7}$	$9.346 \cdot 10^7$	$8.732 \cdot 10^7$	$\mathbf{1.401 \cdot 10^5}$
Utot	0.0719	0.0618	0.2591	0.0578	0.1713	6.4413

Table 4.3: Performance Criteria of control for constant reference signal with disturbances

Performance Criteria	P ZN	PI ZN	PID ZN	PI TL	PID TL	Morari-Zafiriou
ISE	$4.818 \cdot 10^4$	$4.881 \cdot 10^4$	$\mathbf{9.179 \cdot 10^3}$	$4.52 \cdot 10^4$	$1.238 \cdot 10^4$	**14.1529**
IAE	$4.996 \cdot 10^3$	$4.722 \cdot 10^3$	$\mathbf{1.788 \cdot 10^3}$	$5.16 \cdot 10^3$	$2.573 \cdot 10^3$	**32.0007**
ITSE	$7.317 \cdot 10^7$	$6.749 \cdot 10^7$	$\mathbf{1.173 \cdot 10^7}$	$8.65 \cdot 10^7$	$4.078 \cdot 10^7$	$\mathbf{2.713 \cdot 10^3}$
IATE	$4.648 \cdot 10^7$	$4.425 \cdot 10^7$	$\mathbf{2.731 \cdot 10^7}$	$5.808 \cdot 10^7$	$4.33 \cdot 10^7$	$\mathbf{1.591 \cdot 10^5}$
Utot	0.1603	0.1633	0.2870	0.1510	0.2241	0.1645

It can be stated confidently that the Morari-Zafiriou controller outperforms all the others, consistently giving minimum error values, making it the best control choice overall. Furthermore, it is observed that the total control effort (Utot) values stay relatively similar all across the controllers and simulations except the Morari-Zafiriou in the simulation with the variable reference signal. There the Utot of the controller is 6.4413 far above all the other values, indicating that the energy required for control is far greater than on the other controllers.

Chapter 5

Simulations for a Shell-and-tube Heat Exchanger in a feedforward loop

In this chapter, the creation of a feedforward control loop for a shell-and-tube heat exchanger will be conducted. The simulation scenarios, which are going to be analyzed and compared, are the same with the ones observed in chapter 4. In more detail, the construction of the feedforward control loop can be seen in section 5.1, and afterwards a comparison will be made with the best feedback control scheme from chapter 4 in order to determine the best layout for the control of the heat exchanger.

5.1 Feedforward Control System

In this subsection, the mathematical model for the feedforward controller is going to be presented.

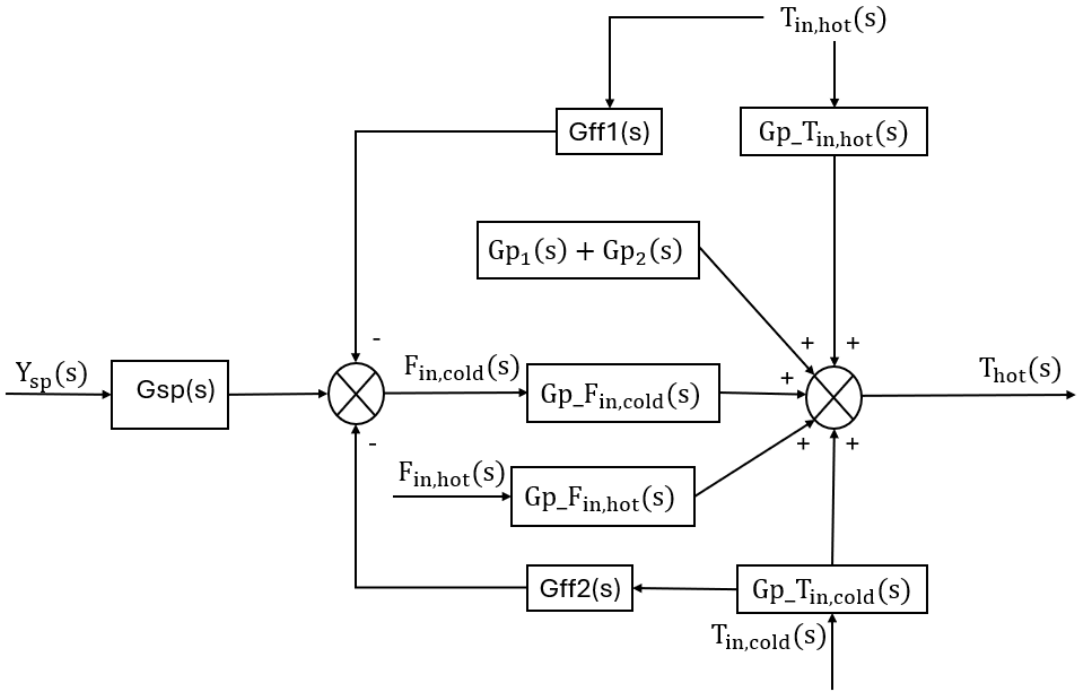

Figure 5.1: Block Diagram of the Feedforward Control System for a Shell-and-Tube Heat Exchanger

The figure 5.1 above shows the block diagram of the feedforward control system. The disturbances present in the figure $F_{in,hot}(s)$, $T_{in,cold}(s)$, $T_{in,hot}(s)$ are the same with chapter 4 and the same applies to their transfer functions as well. Only the transfer functions related to the feedforward control scheme need to be defined (Gff1, Gff2 and

Gsp). Similar to the Morari-Zafiriou methodology at chapter 3, the same principle applies to the process transfer function:

$$\mathrm{Gp}(s) = \mathrm{Gp}^{-}(s) \cdot \mathrm{Gp}^{+}(s) \qquad (5.1)$$

As was previously stated, the first part, $\mathrm{Gp}^{-}(s)$ is called the product of transfer functions that are minimum-phase and essentially reflects the "clean" or desired part. In contrast, the second part, $\mathrm{Gp}^{+}(s)$, is the product of transfer functions that are non-minimum-phase and essentially represents the "undesirable" part. This portion may include:

- Dead time (e.g., an exponential term)
- Zeros in the right half of the complex plane (e.g., in the numerator of the transfer function)
- $|\mathrm{Gp}^{+}(s = i\omega)| = 1$

In the case of the heat exchanger, the process transfer function is purely minimum phase, that is:

$$\mathrm{Gp}(s) = \mathrm{Gp}^{-}(s) = \mathrm{Gp\_F}_{\mathrm{in,cold}}(s) \qquad (5.2)$$

Then the feedforward controller transfer function are as follow:

$$\mathrm{Gsp,min}(s) = \frac{1}{\mathrm{Gp}^{-}(s)} \qquad (5.3)$$

$$\mathrm{G}_{\mathrm{ff1,min}}(s) = \frac{s}{\mathrm{Gp}^{-}(s)} \cdot \left\{\frac{\mathrm{Gp\_T}_{\mathrm{in,hot}}(s)}{s \cdot \mathrm{Gp}^{+}(s)}\right\} \qquad (5.4)$$

$$\mathrm{G}_{\mathrm{ff2,min}}(s) = \frac{s}{\mathrm{Gp}^{-}(s)} \cdot \left\{\frac{\mathrm{Gp\_T}_{\mathrm{in,cold}}(s)}{s \cdot \mathrm{Gp}^{+}(s)}\right\} \qquad (5.5)$$

It is observed that in $\mathrm{Gsp,min}(s)$ the degree of the numerator polynomial is greater than the degree of the denominator polynomial hens the controller is not realizable, to tackle that issue two values are introduced. Just like for the Morari-Zafiriou methodology in chapter 3, λ (lamda) a new parameter for the feedforward controller, which represents a small time constant. An increase in "λ" causes a slower response. Secondly, the exponential term r in the new controller formula, equation (5.9), is the difference between the degree of the denominator polynomial and the degree of the numerator polynomial of Gp(s), where r=2:

$$\mathrm{Gsp}(s) = \frac{1}{\mathrm{Gp}^{-}(s)} \cdot \frac{1}{(\lambda \cdot s+1)^{\mathrm{r}}} \qquad (5.6)$$

$$\mathrm{G}_{\mathrm{ff1}}(s) = \frac{s}{\mathrm{Gp}^{-}(s)} \cdot \left\{\frac{\mathrm{Gp\_T}_{\mathrm{in,hot}}(s)}{s \cdot \mathrm{Gp}^{+}(s)}\right\} \cdot \frac{1}{(\lambda \cdot s+1)^{\mathrm{r}}} \qquad (5.7)$$

$$\mathrm{G}_{\mathrm{ff2}}(s) = \frac{s}{\mathrm{Gp}^{-}(s)} \cdot \left\{\frac{\mathrm{Gp\_T}_{\mathrm{in,cold}}(s)}{s \cdot \mathrm{Gp}^{+}(s)}\right\} \cdot \frac{1}{(\lambda \cdot s+1)^{\mathrm{r}}} \qquad (5.8)$$

Finally, the complete form of the system response is as follows:

$$Y(s) = Gp(s) \cdot [Gsp(s) \cdot Ysp(s) - G_{ff1}(s) \cdot T_{in,hot}(s) - G_{ff2}(s) \cdot T_{in,cold}(s)] + [Gp_1 + Gp_2] + Gp\_F_{in,hot}(s) \cdot F_{in,hot}(s) + Gp\_T_{in,cold}(s) \cdot T_{in,cold}(s) + Gp\_T_{in,hot}(s) \cdot T_{in,hot}(s) \quad (5.9)$$

5.2 Simulation and Comparison of the Feedforward Control System Method

The simulations, as previously stated, are going to be the same with the ones at chapter 4, which are:

- A constant reference signal at 375K.
- A variable reference signal (changes will be made arbitrarily)
- A constant reference signal at 375K and the introduction of the disturbances $T_{in,hot}$, $T_{in,cold}$ (changes will be made arbitrarily)

The detailed changes and values of the variable reference signal as well as the disturbances $T_{in,hot}$ and $T_{in,cold}$ are thoroughly presented in chapter 4.

5.2.1 Simulation for Constant Reference Signal

The response of the feedforward control methodology for a constant reference signal can be observed in this section, with a simulation time up to 10000 seconds.

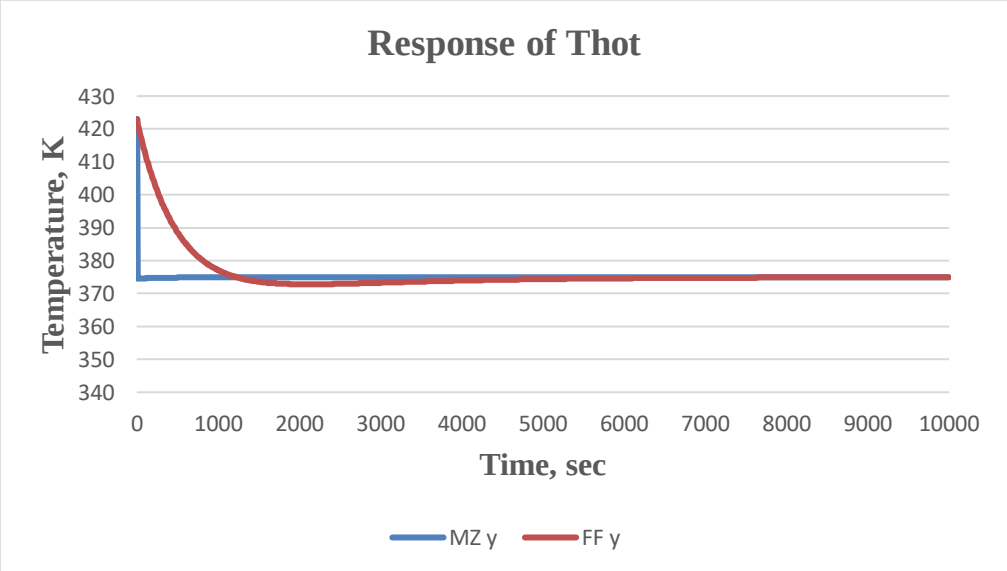

Diagram 5.1: The response of the Thot for the Feedforward system in relation to the Morari-Zafiriou controller

The above diagram 5.1 presents the response of the hot flow temperature of the heat exchanger for the Feedforward control scheme, and it is compared to the Morari-Zafiriou methodology from the previous chapter. It is observed that the Feedforward methodology struggles to reach the predetermined set point as quickly as the Morari-Zafiriou methodology.

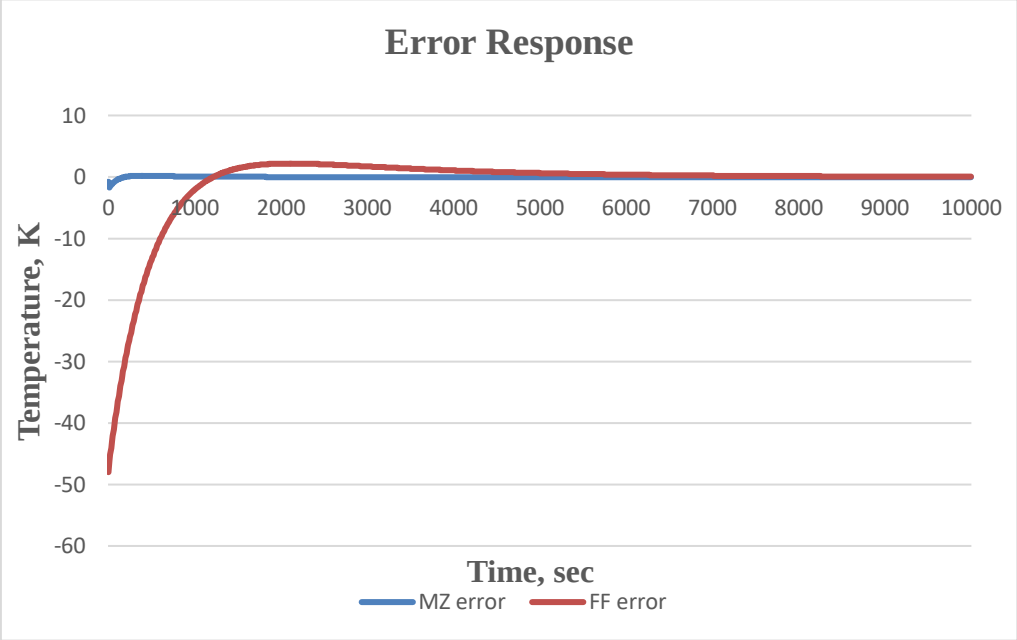

Diagram 5.2: Error exhibited for the Feedforward system in relation to the Morari-Zafiriou controller

Furthermore, in the above diagram 5.2, the error response of the two controllers can be seen. Observing the diagram the conclusion drawn is that the Morari-Zafiriou methodology exhibits error near to zero. In contrast the Feedforward methodology struggles to minimize the error in the first 4000 seconds.

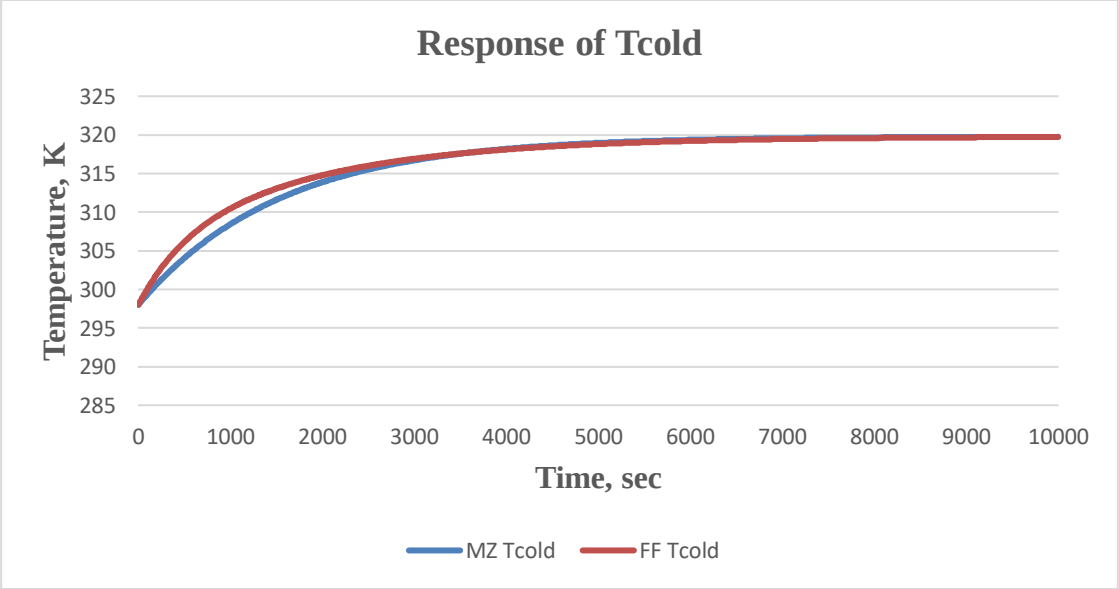

Diagram 5.3: Tcold response for the Feedforward system in relation to the Morari-Zafiriou controller

Finally, diagram 5.3 presents the difference in value regarding the temperature of the cold flow of the heat exchanger. It can be stated that between the Feedforward and Morari-Zafiriou methodologies the values for Tcold are nearly identical.

5.2.2 Simulation for Variable Reference Signal

The second simulation consists of a variable reference signal over the course of 40000 seconds.

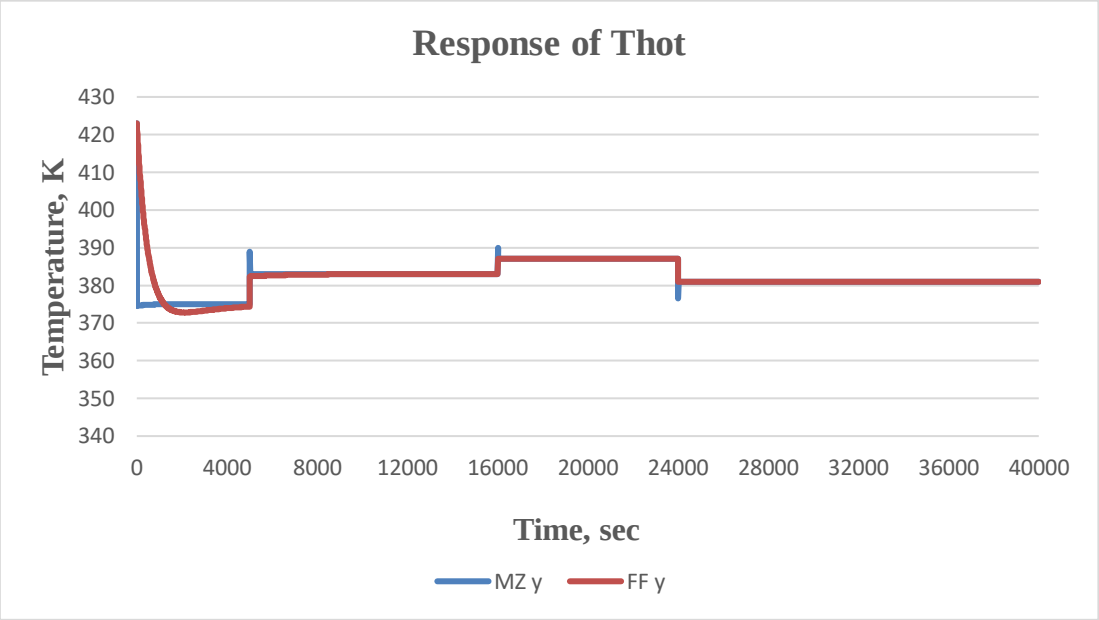

Diagram 5.4: The response of the Thot for the Feedforward system in relation to the Morari-Zafiriou controller

Diagram 5.4 presents the response of the temperature of the hot flow of the heat exchanger. It is observed again that the Feedforward control methodology struggles to reach the predetermined set point at the start of the simulation, in contrast to the Morari-Zafiriou methodology, which reaches the reference signal near instantaneously. Nevertheless, as shown in the diagram the Feedforward controller performs better when it comes to changes in the signal, by instantly adapting without straying.

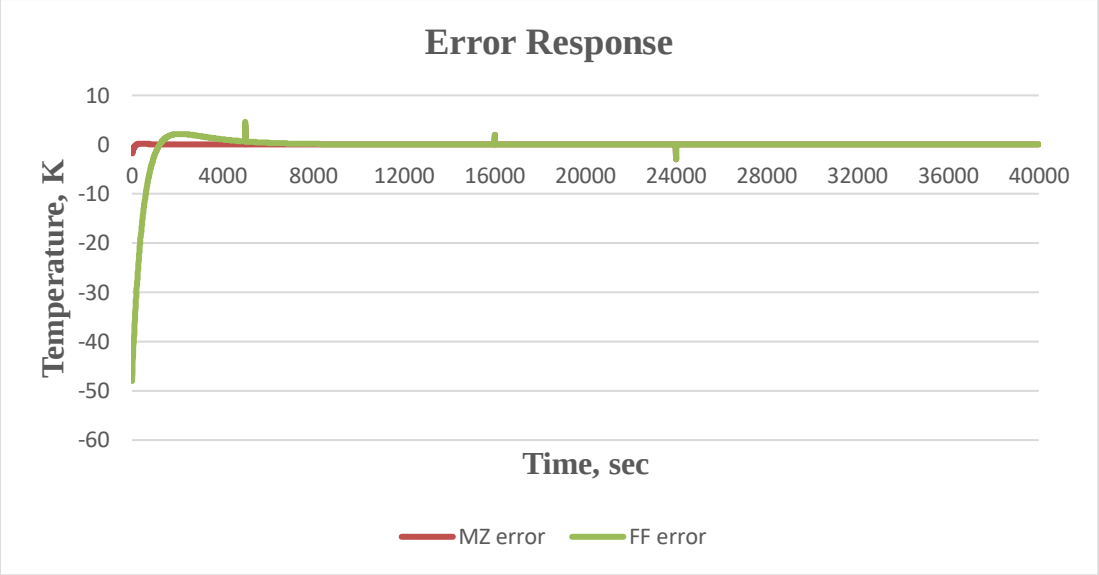

Diagram 5.5: Error exhibited for the Feedforward system in relation to the Morari-Zafiriou controller

In the diagram above the error values of the two methodologies for a variable reference signal are shown. There it can be observed more clearly the straying that the Morari-Zafiriou methodology does when a change to the signal is made, as well as the slower response of the Feedforward control methodology at the start of the simulation.

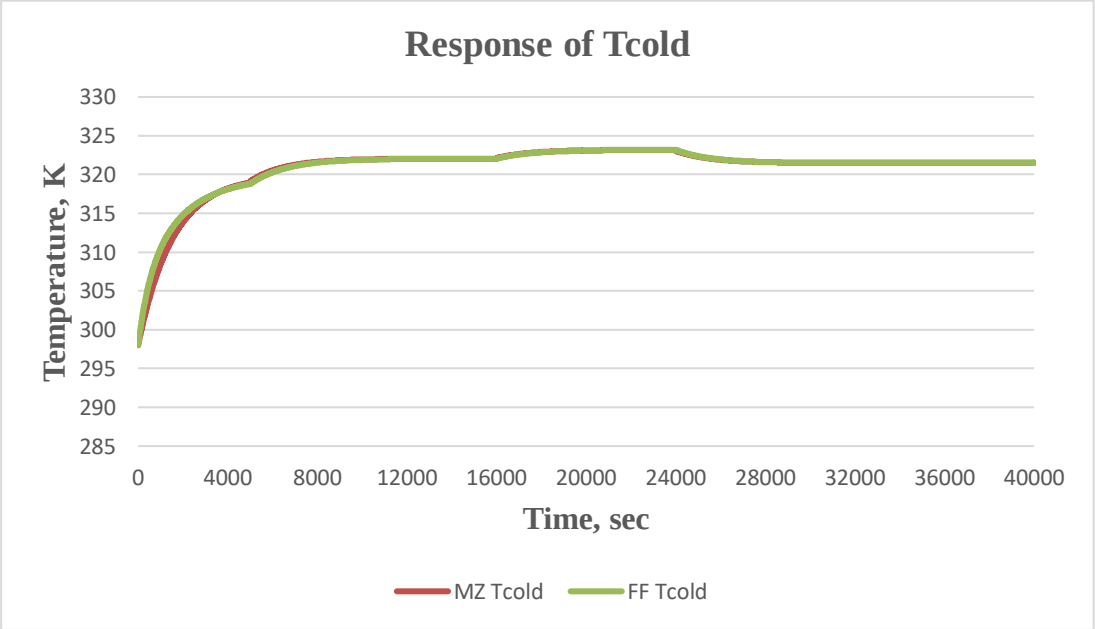

Diagram 5.6: Tcold response for the Feedforward system in relation to the Morari-Zafiriou controller

Finally, diagram 5.6 presents the difference in value regarding the temperature of the cold flow of the heat exchanger. It can be again stated that between the Feedforward and Morari-Zafiriou methodologies the values for Tcold are nearly identical.

5.2.3 Simulation for a constant reference signal and the introduction of the disturbances $T_{in,hot}$, $T_{in,cold}$

The third simulation consists of a constant reference signal at 375 K and the introduction of two disturbances $T_{in,hot}$, $T_{in,cold}$.

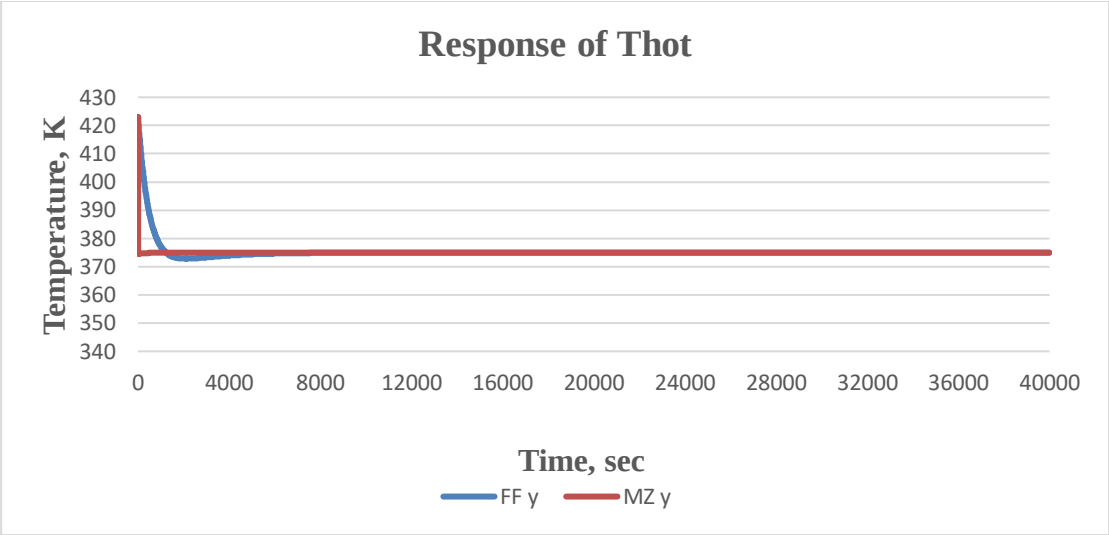

Diagram 5.7: The response of the Thot for the Feedforward system in relation to the Morari-Zafiriou controller

Diagram 5.7 presents the response of the temperature of the hot flow of the heat exchanger. It is observed again that the Feedforward control methodology struggles to reach the predetermined set point at the beginning of the simulation, in contrast to the Morari-Zafiriou methodology, which reaches the reference signal near instantaneously. Additionally, the disturbances that were introduced to the system seem to not affect the response of Thot for either controller.

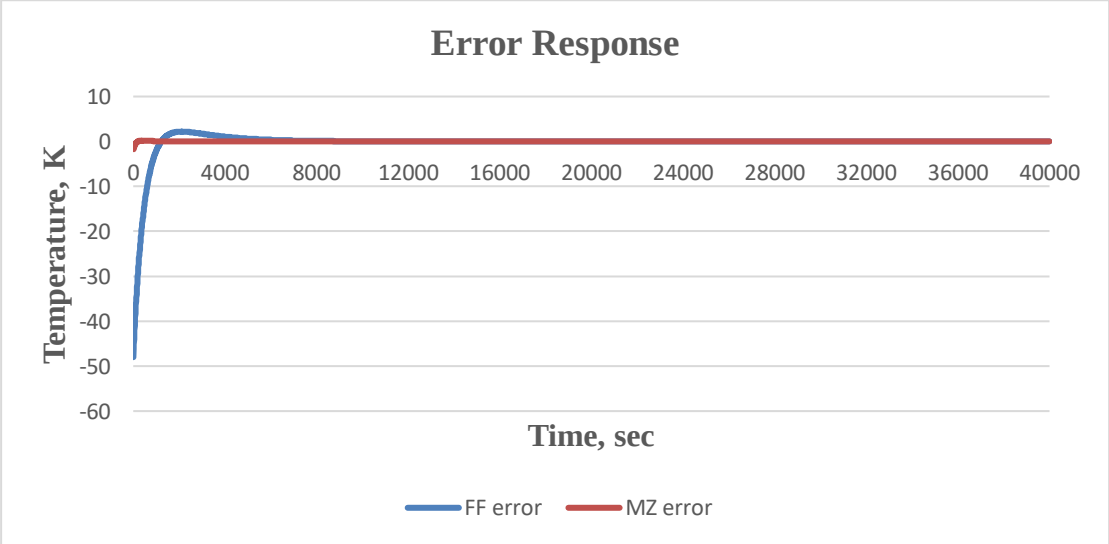

Diagram 5.8: Error exhibited for the Feedforward system in relation to the Morari-Zafiriou controller

Furthermore, in the above diagram 5.8, the error response of the two controllers can be seen. Observing the diagram the conclusion drawn is that the Morari-Zafiriou methodology exhibits error near to zero. In contrast the Feedforward methodology struggles to minimize the error in the first 4000 seconds.

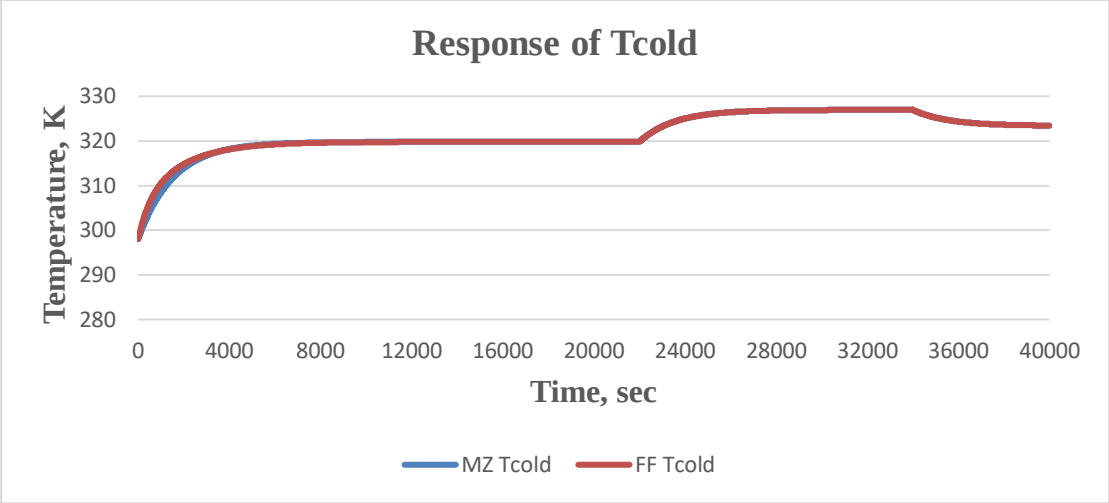

Diagram 5.9: Tcold response for the Feedforward system in relation to the Morari-Zafiriou controller

Lastly, in diagram 5.9 the difference in value regarding the temperature of the cold flow of the heat exchanger is presented. It can be again stated that between the Feedforward and Morari-Zafiriou methodologies the values for Tcold are nearly identical.

5.2.4 Comparison of the two types of controllers

In this section, a variety of performance criteria are used to evaluate the efficiency and effectiveness of the controllers for each simulation scenario.

Table 5.1: Performance Criteria of control for constant reference signal

Performance Criteria	Feedforward	Morari-Zafiriou
ISE	$4.7195 \cdot 10^4$	**14.3992**
IAE	$2.4094 \cdot 10^3$	**26.2201**
ITSE	$1.0951 \cdot 10^7$	**$1.359 \cdot 10^3$**
IATE	$2.8781 \cdot 10^6$	**$1.353 \cdot 10^4$**
Utot	0.1234	0.1410

Table 5.2: Performance Criteria of control for variable reference signal

Performance Criteria	Feedforward	Morari-Zafiriou
ISE	$4.7229 \cdot 10^4$	**43.4001**
IAE	$2.4184 \cdot 10^3$	**35.4005**
ITSE	$1.1336 \cdot 10^7$	**$3.614 \cdot 10^5$**
IATE	$3.0022 \cdot 10^6$	**$1.401 \cdot 10^5$**
Utot	28.1109	**6.4413**

Table 5.3: Performance Criteria of control for constant reference signal with disturbances

Performance Criteria	Feedforward	Morari-Zafiriou
ISE	$4.7195 \cdot 10^4$	**14.1529**
IAE	$2.4111 \cdot 10^3$	**32.0007**
ITSE	$1.0951 \cdot 10^7$	**$2.713 \cdot 10^3$**
IATE	$2.9341 \cdot 10^6$	**$1.591 \cdot 10^5$**
Utot	0.1468	0.1645

Concluding the comparison, the Morari-Zafiriou controller outperforms the Feedforward, consistently giving minimum error values, making it the best control choice between the two. Furthermore, it is observed that the total control effort (Utot) values stay relatively among the two except the simulation with the variable reference signal. There the Utot of the Morari-Zafiriou controller is 6.4413 and the Feedforward is 28.1109 far above the values of the other two simulation scenarios, indicating that the system needs a greater amount of energy for control, especially for the Feedforward methodology.

Chapter 6

Conclusions

The core aim of this paper was the comparison of different control methodologies that can be applied to a shell-and-tube heat exchanger. Additionally, a mathematical analysis followed as well as the linearization of the system using Taylor-Series, the State Space Model and the Laplace Transform. Subsequently, some important aspects of Control Systems were presented in a theoretical background, the methodologies of Ziegler–Nichols and Tyreus-Luyben were used in the tuning of the P, PI and PID controllers as well as the Model based or Morari-Zafiriou control methodology for the implementation of six different types of controllers for the closed-loop system. Furthermore, three different simulation scenarios were developed for the comparison of the controllers, a steady set point, a variable set point and a steady set point with two disturbances. Based on the data drawn from the simulations, the best controller was found to be the one derived from the Morari–Zafiriou methodology. This specific controller acts quickly and appropriately on the system, so that the response of the heat exchanger reaches the reference signal in any simulation with minimal error values. Second was the PID controller from the Ziegler–Nichols methodology, it was observed that this controller reaches the reference signal in a slower manner compared to the Morari–Zafiriou with some oscillation present. On the other hand, it functions with smaller overall error values than its Tyreus-Luyben counterpart. In addition, the P and PI controllers for both Methodologies were found to exhibit similar behaviors in the simulations, due to their oscillatory responses. However, the PI controllers were better, since they do not produce errors as large as those of the P controller. Afterwards the best controller of the feedback loop was compared to a controller from an entirely different layout. The introduction of the feedforward control strategy followed. The feedforward controller was tested under the same simulation scenarios as the other six controllers. The results yielded from the simulations point that the better controller among the two was the Morari-Zafiriou. Future studies regarding the effective control of shell-and-tube heat exchangers should involve the application of cascade or feedback-feedforward control strategies. Other advanced methodologies such as model predictive control or neural network control can also be used. Lastly the effectiveness of all those control strategies have to be tested in a lab format to verify the results given by the simulations.

References

[1] Z. Anxionnaz, M. Cabassud, C. Gourdon, and P. Tochon, “Heat exchanger/reactors (HEX reactors): Concepts, technologies: State-of-the-art,” *Chemical Engineering and Processing: Process Intensification*, vol. 47, no. 12. pp. 2029–2050, Nov. 2008. doi: 10.1016/j.cep.2008.06.012.

[2] P. Kapustenko, S. Boldyryev, O. Arsenyeva, and G. Khavin, “The use of plate heat exchangers to improve energy efficiency in phosphoric acid production,” *Journal of Cleaner Production*, vol. 17, no. 10, pp. 951–958, Jul. 2009, doi: 10.1016/j.jclepro.2009.02.005.

[3] S. Lv *et al.*, “Study of different heat exchange technologies influence on the performance of thermoelectric generators,” *Energy Conversion and Management*, vol. 156, pp. 167–177, Jan. 2018, doi: 10.1016/j.enconman.2017.11.011.

[4] D. S. Patil, R. R. Arakerimath, and P. v. Walke, “Thermoelectric materials and heat exchangers for power generation – A review,” *Renewable and Sustainable Energy Reviews*, vol. 95. Elsevier Ltd, pp. 1–22, Nov. 01, 2018. doi: 10.1016/j.rser.2018.07.003.

[5] S. Padhee, “Controller Design for Temperature Control of Heat Exchanger System: Simulation Studies.”

[6] S. I. . Ao, *World Congress on Engineering : WCE 2010 : 30 June - 2 July, 2010, Imperial College London, London, U.K.* Newswood Ltd. : International Association of Engineers, 2010.

[7] R. Ranjan and S. Kumar, “An Efficient Cascaded Effect Based Parallel Flow Heat Exchanger Using Nonlinear Model Predictive Controller Based Fuzzy Optimization Technique,” *Arabian Journal for Science and Engineering*, vol. 48, no. 3, pp. 3227–3239, Mar. 2023, doi: 10.1007/s13369-022-07120-w.

[8] E. Tridianto, T. H. Ariwibowo, S. K. Almasa, and H. E. G. Prasetya, “Cascaded PID temperature controller for FOPDT model of shell-and-tube heat exchanger based on Matlab/Simulink,” in *Proceedings IES-ETA 2017 - International Electronics Symposium on Engineering Technology and Applications*, Institute of Electrical and Electronics Engineers Inc., Dec. 2017, pp. 185–191. doi: 10.1109/ELECSYM.2017.8240400.

[9] R. Dyrska, M. Horváthová, P. Bakaráč, M. Mönnigmann, and J. Oravec, “Heat exchanger control using model predictive control with constraint removal,” *Applied Thermal Engineering*, vol. 227, Jun. 2023, doi: 10.1016/j.applthermaleng.2023.120366.

[10] L. Liu, S. Tian, D. Xue, T. Zhang, and Y. Q. Chen, “Industrial feedforward control technology: a review,” *Journal of Intelligent Manufacturing*, vol. 30, no. 8, pp. 2819–2833, Dec. 2019, doi: 10.1007/s10845-018-1399-6.

[11] Y. Fürst, S. Brandt, and M. Kriegel, “Introducing a new nonlinear approach to model heat exchangers designed for control engineering applications,” *European Journal of Control*, vol. 79, Sep. 2024, doi: 10.1016/j.ejcon.2024.101072.

[12] B. Tomar, N. Kumar, and M. Sreejeth, “PLC and SCADA based temperature control of heat exchanger system through fractional order PID controller using metaheuristic optimization techniques,” *Heat and Mass Transfer/Waerme- und Stoffuebertragung*, vol. 60, no. 9, pp. 1585–1602, Sep. 2024, doi: 10.1007/s00231-024-03509-5.

[13] G. M. Sarabeevi and M. L. Beebi, “Temperature control of shell and tube heat exchanger system using internal model controllers,” in *2016 International Conference on Next Generation Intelligent Systems (ICNGIS)*, IEEE, Sep. 2016, pp. 1–6. doi: 10.1109/ICNGIS.2016.7854015.

[14] U. U. Rehman, “Heat Transfer Optimization of Shell-and-Tube Heat Exchanger through CFD Studies.”

[15] “Balance Equations.” http://apmonitor.com/pdc/index.php/Main/PhysicsBasedModels (accessed Mar. 12, 2021).

[16] S. Padhee, Y. B. Khare, and Y. Singh, “Internal model based PID control of shell and tube heat exchanger system,” in *IEEE Technology Students’ Symposium*, IEEE, Jan. 2011, pp. 297–302. doi: 10.1109/TECHSYM.2011.5783833.

Greek References (Books): [17]-[19]

[17]Πουλιέζος Αναστάσιος, Περί συστημάτων ελέγχου. Αθήνα: Τζιόλα, 2013.

[18]D. G. S. Charles E. Rohrs, James L. Melsa, Γραμμικά συστήματα αυτόματου ελέγχου. Τζιόλα, 1996.

[19]Κωνσταντίνου Κωνσταντίνος, “ΑΝΩΤΑΤΟ ΤΕΧΝΟΛΟΓΙΚΟ ΕΚΠΑΙΔΕΥΤΙΚΟ ΙΔΡΥΜΑ ΚΡΗΤΗΣ ΠΑΡΑΡΤΗΜΑ ΧΑΝΙΩΝ ΤΜΗΜΑ ΗΛΕΚΤΡΟΝΙΚΗΣ ΘΕΜΑ «Μελέτη Αναλογικών, Ψηφιακών και Προγραμματιζόμενων Ελεγκτών»,” ΑΝΩΤΑΤΟ ΤΕΧΝΟΛΟΓΙΚΟ ΕΚΠΑΙΔΕΥΤΙΚΟ ΙΔΡΥΜΑ ΚΡΗΤΗΣ ΠΑΡΑΡΤΗΜΑ ΧΑΝΙΩΝ ΤΜΗΜΑ ΗΛΕΚΤΡΟΝΙΚΗΣ, 2012.

[20]S. Yehia, “Applying heat exchanger control strategies,” Control Eng., vol. 63, no. 1, pp. P1–P6, Jan. 2016.

[21]“Basic Feedback Control Principles | Closed-loop Control Systems | Automation Textbook.” https://control.com/textbook/closed-loop-control/basic-feedback-control-principles/ (accessed Mar. 13, 2021).